Optimal Control Prediction Method for Control Allocation

Michael J. Acheson*
NASA Langley Research Center, Hampton, VA, 23681

This paper proposes a novel prediction method for online optimal control allocation that extends the volume of moments achievable with the Moore-Penrose generalized inverse to the entire Attainable Moment Set. This method formulates the control allocation problem using selected basis vectors and associated gains which reduces the optimization problem dimensions and provides physical insight into the resulting optimal solutions. The proposed algorithm finds the entire family of unique optimal control solutions along the desired moment vector from the origin to the boundary of the Attainable Moment Set. Numerical results for the Moore-Penrose prediction method show that the unique minimal controls obtained yield the desired moment with near machine precision accuracy while maintaining control effectors within specified position limits. This method has been fully validated against the unique solution obtained on the boundary of the Attainable Moment Set using the Durham Direct Allocation method. Minimal control solutions obtained for moments in the interior of the Attainable Moment Set, similarly yield the desired moment to near machine precision while providing control solutions that are smaller (i.e. 2-norm) than solutions found with traditional control allocation algorithms (e.g. interior point methods) applied to the minimal control problem. Numerical simulations using a Matlab® autocoded executable (MEX) for the representative real world problem of 3-moments with 20 individual control effectors and prescribed control position limits show a mean computation speed of approximately 125 Hz which is sufficient to enable real-time flight allocation.

I. Nomenclature

$\delta(\Omega)$	=	boundary of Allowable Control Set
$\delta(\Phi)$	=	boundary of Attainable Moment Set
Γ	=	Gain subspace for null-space basis vectors, $\Gamma \subset \Re^{m-n}$
Ω	=	Allowable Control Set (ACS), $\Omega \subset \Re^m$
Φ	=	Attainable Moment Set (AMS), $\Phi \subset \Re^n$
ACS	=	Allowable Control Set, Ω
AMS	=	Attainable Moment Set, Φ
B	=	control effectiveness matrix, $B \in \Re^{n\times m}$
$\hat{\mathcal{B}}$	=	complete orthogonal basis vector matrix containing $\hat{u}_{des}$ and $\mathcal{N}(B)$ basis vectors
$\hat{B}$	=	orthogonal basis vector matrix containing $\mathcal{N}(B)$ basis vectors
$\vec{m}_{des}$	=	desired moment, $\vec{m}_{des} \in \Re^n$
$\hat{m}_{des}$	=	unit vector in the direction of desired moment, $\hat{m}_{des} \in \Re^n$
P_{Iso}	=	Moore-Penrose Iso surface, orthogonal projection of ACS on $\mathcal{N}(B)$
P_{min}	=	Moore-Penrose generalized inverse of control effectiveness matrix B, $P_{min} \in \Re^{m\times n}$
$\mathcal{P}_{P_{min}}$	=	Orthogonal projection operator onto Moore-Penrose surface
P_{Smin}	=	Moore-Penrose surface, orthogonal projection of ACS on span of P_{min} column vectors
$\vec{r}_{lwr}$	=	Lower bounds of control effector rate limitations, $\vec{r}_{lwr} \in \Re^m$
$\vec{r}_{upr}$	=	Upper bounds of control effector rate limitations, $\vec{r}_{upr} \in \Re^m$
S_1	=	Set of indices for all currently unsaturated control effectors, $S_1 = \{1, 2, \ldots, m\} \setminus S_2$
S_2	=	Set of indices for all currently saturated control effectors (e.g. $S_2 = \{1, 5, 10\}$)
$\vec{s}_2$	=	Vector of active control effectors position limits for all indices in S_2

*NASA Researcher, Dynamics Systems and Controls Branch, NASA Langley Research Center, michael.j.acheson@nasa.gov, AIAA Member

$\hat{u}_{des}$ = Control unit vector in the direction of $P_{min}\vec{m}_{des}$, $\hat{u}_{des} \in \Re^m$
$\vec{u}_{lwr}$ = Lower bounds of control effector position limitations, $\vec{u}_{lwr} \in \Re^m$
$\vec{u}_{opt}$ = Optimal control allocation solution, $\vec{u}_{opt} \in \Re^m$
$\vec{u}_{upr}$ = Upper bounds of control effector position limitations, $\vec{u}_{upr} \in \Re^m$
W_{gi} = Positive definite weighting matrix used for generation of arbitrary generalized inverse, $W_{gi} \in \Re^{m \times m}$

II. Introduction

Historically, the aircraft control problem has been segregated along individual axes and flight controls were "ganged" such that specific control effector groupings were assigned to control individual axes. Conversely, many modern control approaches make use of control allocation or the process of ungrouping all control effectors to collectively provide the desired control across all axes simultaneously. More specifically, since modern aircraft have more control effectors than desired outcomes, typical control allocation methods seek to solve an over-determined system of linear equations and thereby find control effector deflections within the Attainable Control Set (ACS) to achieve the specified control moments (e.g. angular accelerations) within the Attainable Moment Set (AMS). Modern flight control seeks to implement real-time control allocation methods for many reasons including: control efficiency, increased utilization of the ACS, increased capability to achieve any desired control moment in the AMS, an inherent ability to accommodate control failures and the promise of accomplishing secondary objectives (e.g. minimize drag, avoid structural modes) while simultaneously performing desired flight control.

Early methods of real-time control allocation were severely limited due to the substantial computational burden of solving systems with dimensions relevant to modern flight vehicles. As a result, ad-hoc or limited methods were applied which had severe limitations such as: provided true optimal controls allocation solutions in known limited situations, could only reach portions of moment space (Attainable Moment Set), would provide optimal or non-optimal control allocation solutions on an unpredictable basis, or compromised solution accuracy for computational efficiency. Some legacy methods for controls allocation include Direct Allocation, Redistributed Pseudo-Inverse, Quadratic Programming and Linear Programming. [1–3] The limitations of the legacy control allocation methods have very substantial consequences especially in light of modern unstable/marginally unstable aircraft designs. For example, the ability to consistently achieve Moore-Penrose (minimum control) allocation solutions $\forall \vec{m}_{des} \in \Phi$ for an all electric aircraft has the promise to substantially increase battery life. The inability to achieve attainable moments near the boundaries of the AMS have dire consequences to an aircraft in out-of-controlled flight whose flight allocation routine fails to provide sufficient control authority to recover.

In contrast, the proposed Prediction Method (PM) in this paper reformulates the allocation problem for systems of non-redundant controls and provides proven analytic optimal solutions for both the Moore-Penrose and arbitrary (weighted) generalized inverse along any desired moment direction. This work therefore guarantees optimal control allocation solutions throughout the entire AMS and does so with a predictable and tractable computational burden. Finally, the PM method readily accommodate changes to the dimensions of the controls effectiveness matrix (B) which addresses some actuator failure modes.

III. Background

Typical methods of addressing the controls allocation problem can be categorized into offline and online approaches. Offline approaches require apriori knowledge of the linear controls effectiveness matrix (B matrix) but they offer the advantage that much of the heavy computational work is done before use and therefore solution generation during execution is greatly simplified (e.g. matrix vector multiplication). The requirement to have knowledge of the controls effectiveness B matrix, hinders an offline method's ability to accommodate control effector failures or to work with changing controls effectiveness matrices due to online system identification routines. Conversely online methods remove the requirement to have a priori knowledge of the controls effectiveness B matrix but generally suffer in solution accuracy and/or computational burden.

Generalized inverses, which are closely related to the primary area of study in this paper, have been utilized historically both offline and online. A generalized inverse P_{gi} (e.g. Moore-Penrose pseudo-inverse P_{min}) offers a constant matrix optimal control allocation solution to the inverse problem: $\vec{u}_{opt} = P_{gi}\vec{m}_{des}$ which ensures that $B\vec{u}_{opt} = \vec{m}_{des} \coloneqq B\left(P_{gi}\vec{m}_{des}\right)$. The main criticism of the offline generalized inverse approach is that the moments achievable, while maintaining control effectors within position limits, are always limited to a subset of the Attainable Moment Set (Φ). In fact, for a given B matrix and control effector position limits ($\vec{u}_{lwr}, \vec{u}_{upr}$), Durham [1] and

Bordignon [4] note that no weighted generalized inverse exists which can achieve optimal control allocation solutions $\forall \vec{m} \in \Phi$. Durham and Bordignon proposed a "best generalized inverse" which maximized the subset of the AMS volume for which the best generalized inverse would provide control solutions within effector position limits. While limited in applicability in Φ, the use of a constant matrix generalized inverse facilitates linear stability analysis which is often desired or required. Online generalized inverse methods (e.g. Redistributed Pseudo Inverse or Cascading Generalized Inverse) typically attempt to address the inability of any single generalized inverse to yield optimal control allocation solutions $\forall \vec{m} \in \Phi$. This is usually accomplished in an iterative fashion: computing a generalized inverse, determining which control effectors are saturated, removing them from consideration, recomputing a generalized inverse for the set of unsaturated controls and repeating as necessary. While these online generalized inverse methods are fast, they provide no guarantee of yielding an optimal control allocation solution nor do they provide solutions $\forall \vec{m} \in \Phi$ [4] [5] The Null-Space Intersection method utilizes the null-space of the controls effectiveness matrix B to restore a control allocation solution which violates control effector position limits back within the Allowable Control Set. [4] The method involves finding the intersection of a subspace with a higher dimension polytope. However, due to the very high number of objects to search and numerical difficulties, this method was relegated by Bordignon as a research tool with little potential for real world application. Bordignon and Bessolo have had good success success using the Cascading Generalize Inverse (CGI) method for control allocation on a modern front-line fighter prototype aircraft, the X-35B [6].

Furthermore, a literature survey shows wide variations in how the aforementioned control allocation methods define and set up the control allocation problem. A seminal paper by Durham [1] defined control allocation as determining the unique optimal control allocation solution yielding the maximum available moment on the AMS boundary in the direction of a desired moment and simply scaling this control solution (non-optimal) for any desired interior moment. Enns [3] defines control allocation based on the types of solutions to the linear system. In the case of no solutions, control allocation is to "approximately solve" or minimize $1/2(B\vec{u} - \vec{d})^T W_d (B\vec{u} - \vec{d})$ with $W_d > 0$. For the case of infinite solutions, he defines control allocation as solving $B\vec{u} = \vec{d}$ while also minimizing $1/2(\vec{u} - \vec{u}_p)^T W_d (\vec{u} - \vec{u}_p)$ with $W_p > 0$ and $\vec{u}_p$ the preferred result. Davidson et al. [7] define the basic control allocation definition as solving $\vec{m}_d = B\delta$ with constrained δ using the weighted pseudo-inverse solution as $J = 1/2\delta^T W\delta + \lambda^T(\vec{m}_d - B\delta)$ with $W > 0$. Bodson [5] examines the basic controls allocation problem of $(CB)\vec{u} = \vec{a}_d$ with $\vec{u}$ subject to position constraints, and examines four formulations of the solutions: direct allocation formulation as stated by Durham, error minimization as $J = \|CB\vec{u} - \vec{a}_d\|$, control minimization as given $\vec{u}_p$, $\vec{u}_1$ then find $\vec{u}$ such that $J = \left\|\vec{u} - \vec{u}_p\right\|$ is minimized subject to $(CB)\vec{u} = (CB)\vec{u}_1$ and mixed optimization problem given $\vec{u}_p$ then minimize $J = \|CB\vec{u} - \vec{a}_d\| + \epsilon \left\|\vec{u} - \vec{u}_p\right\|$. A current control allocation definition by Durham et al. [8] requires that the original problem $B\vec{u}_{opt} = \vec{m}_{des}$ is solved, but for interior cases with infinite solutions they define the concept of a "preferred solution". This concept allows freedom in selecting the optimal or preferred control solution among the infinite choices.

This wide variety of historical definitions of control allocation, motivates a more universal definition closely aligned with the arbitrary generalized inverse. This proposed definition of optimal control allocation, as defined in this paper, is finding the unique control solution within the entire AMS (in the interior or on the AMS boundary) which satisfies the desired moment or if not attainable then the maximal moment in the direction of the desired moment, while simultaneously providing the minimum weighted control cost. Given $W_{gi} \in \Re^{m \times m}$ where $W_{gi} > 0$ then generalized inverse optimal controls allocation is defined as determining $\vec{u}$ such that:

$$\begin{aligned} &\min_{\vec{u}} J(\vec{u}) \coloneqq \vec{u}^T W_{gi} \vec{u} \text{ such that } B\vec{u}_{opt} = \vec{m}_{des} \text{ and} \\ &\vec{u}_{min} \leq \vec{u}_{opt} \leq \vec{u}_{max}, \quad \vec{r}_{min} \leq \frac{d}{dt}\vec{u}_{opt} \leq \vec{r}_{max} \end{aligned} \tag{1}$$

where $\vec{u}_{min}$ and $\vec{u}_{max}$ are the minimal and maximal control effector position limitation vectors, and the vectors $\vec{r}_{min}$, $\vec{r}_{max}$ are the minimal and maximal control effector rate limitation vectors. This formulation is shown to be closely aligned with the definition of an arbitrary generalized inverse [6]:

$$P_{gi} \coloneqq W_{gi}^{-1} B^T \left(B W_{gi}^{-1} B^T\right)^{-1} \tag{2}$$

The requirement for $W_{gi} > 0$ can be relaxed to $W_{gi} \geq 0$ and then the arbitrary generalized inverse can be defined as:

$$P_{gi} \coloneqq W_{gi} B^T \left(B W_{gi} B^T\right)^{-1} \tag{3}$$

but the remainder of the definition for optimal control allocation in Eq. (1) remains the same. Similarly, the special case of Moore-Penrose (MP) optimal control allocation seeks to find the minimum 2-norm control magnitude, and thus the

MP optimal control allocation (with $W_{gi} = I$) is defined in this paper as:

$$\min_{\vec{u}} J(\vec{u}) \coloneqq \vec{u}^T \vec{u} \text{ such that } B\vec{u}_{opt} = \vec{m}_{des} \text{ and} \tag{4}$$
$$\vec{u}_{min} \leq \vec{u}_{opt} \leq \vec{u}_{max}, \quad \vec{r}_{min} \leq \frac{d}{dt}\vec{u}_{opt} \leq \vec{r}_{max}$$

which is closely associated with the MP generalized inverse::

$$P_{min} \coloneqq B^T \left(BB^T\right)^{-1} \tag{5}$$

While not expounded upon in this paper (instead handled in a separate treatise), there is certainly a valid argument to include the concept of a preferred control vector $\vec{u}_p$ in the general definition found in Eq. (1), which would yield:

$$\min_{\vec{u}} J(\vec{u}) \coloneqq \left(\vec{u} - \vec{u}_p\right)^T W_{gi} \left(\vec{u} - \vec{u}_p\right) \text{ such that } B\vec{u_{opt}} = \vec{m}_{des} \text{ and} \tag{6}$$
$$\vec{u}_{min} \leq \vec{u}_{opt} \leq \vec{u}_{max}, \vec{r}_{min} \leq \frac{d}{dt}\vec{u}_{opt} \leq \vec{r}_{max}$$

A simple example of one such supporting case would be to utilize $\vec{u}_p$ to establish the longitudinal trim of an aircraft stabilator.

Further explanation of the relationship between the novel online prediction method of this paper and the definitions of Eqs. (1-5) is warranted. In essence, the online prediction method formulates a simplified problem that minimizes $J(\vec{u}) \coloneqq \vec{u}^T W_{gi} \vec{u}$ and satisfies $B\vec{u_{opt}} = \vec{m}_{des}$ in an iterative algorithm as successive control effectors saturate. Based on the geometry of the subspaces, only the portion of $\vec{u}_{opt}$ in the $\mathcal{N}(B)$ requires optimization at each iteration. This local optimization is performed as the desired moment vector $\vec{m}_{des}$ is increased from the origin to the boundary of the Attainable Moment Set (AMS) along a specified moment unit vector direction $\hat{m}_{des}$. In this way, the online prediction method finds the entire family of optimal control allocation solutions along $\hat{m}_{des}$.

It is the author's opinion, that there is utility in a controls allocation definition that consistently produces a unique optimal control allocation solution $\forall \vec{m}_{des} \in \Phi$. An aircraft in flight should always maintain state awareness of the optimal allocation solution for use to the largest extent practical, while maintaining the freedom to utilize other preferred solutions (non-optimal) as needed.

IV. Prediction Method Algorithm Description

A. Moore Penrose Control Allocation Problem Formulation

The typical linear control effectiveness matrix (B) and arbitrary control vector ($\vec{u}$) matrix multiplication $B\vec{u} = \vec{m}$ effectively divides the control space into two orthogonal subspaces that have great importance in solving the Moore-Penrose (MP) control allocation problem. In simple form, the matrix vector operation divides $\vec{u}$ as follows:

$$\vec{u} = \vec{u}_{\parallel} + \vec{u}_{\perp} \implies B\vec{u} = B\vec{u}_{\parallel} + B\vec{u}_{\perp} = B\vec{u}_{\parallel} = \vec{m} \tag{7}$$

The vector $\vec{u}_{\parallel}$ is obtained by an orthogonal projection ($\mathcal{P}_{P_{min}}$) of $\vec{u}$ onto the Moore Penrose (MP) subspace which is a first subspace of $\Re^m$. We know from linear algebra the matrix product of $B\vec{u}$ is equivalent to the composition of the controls effectiveness matrix B with the orthogonal projection operator ($\mathcal{P}_{P_{min}}$) onto the MP subspace and therefore $B\vec{u} = B \circ \mathcal{P}_{P_{min}}\vec{u} = \vec{u}_{\parallel}$. Also from linear algebra we know that $\vec{u}_{\perp}$ resides in the kernel or null-space $\mathcal{N}(B)$, which is the second subspace of $\Re^m$. As $\vec{u}_{\perp} \in \mathcal{N}(B)$, then $B\vec{u}_{\perp}$ makes no contribution to $\vec{m}$ and therefore the matrix vector multiplication $B\vec{u}$ effectively operates solely on $\vec{u}_{\parallel}$.

For the unconstrained $\vec{u}$ case, $\vec{u}_{\parallel}$ be any vector in the MP subspace. However, for constrained $\vec{u}$, $\vec{u}_{\parallel}$ is limited to a subset of the MP subspace (defined as the MP surface P_{Smin} in this paper) and $\vec{u}_{\parallel}$ is used to satisfy $\vec{m}_{des}$ while $\vec{u}_{\perp}$ becomes essential in satisfying control position constraints. For this paper, the MP Iso surface P_{Iso} is a subset of the subspace $\mathcal{N}(B)$ in which $\vec{u}_{\perp}$ resides and it contains the components of $\vec{u}$ which make no contribution to or equivalently maintain a constant (iso) moment $\vec{m}$.

Some basic definitions are in order. The Allowable Control Set is defined as:

$$\Omega \coloneqq \{\vec{u} \in \Re^m | \vec{u}_{lwr_i} \leq \vec{u}_i \leq \vec{u}_{upr_i}, \forall i \in \{1, 2, \ldots m\}\} \tag{8}$$

The Attainable Moment Set (Φ) (as defined by Durham [1]) is the closed and bounded set generated by B-mapping the closed and bounded Allowable Control Set (Ω).

$$\Phi \coloneqq \{\vec{m} \in \Re^n | B\vec{u} = \vec{m}, u \in \Omega\} \subset \Re^n \tag{9}$$

Recalling the definition of the null space $\mathcal{N}(B)$ of a matrix as:

$$\mathcal{N}(B) \coloneqq \{\vec{u} \in \Re^m \mid B\vec{u} = \vec{0}, \text{ given } B \in \Re^{n\times m}\}$$

then the Moore-Penrose (MP) surface (P_{Smin}) and Iso-surface (P_{Iso}) are defined as follows:

$$\begin{aligned} P_{Smin} &\coloneqq \{\vec{u} : \vec{u} = P_{min}\vec{m}, \vec{m} \in \Phi\} \equiv \\ &\coloneqq \{\mathcal{P}_{P_{min}}\vec{u} | \vec{u} \in \Omega\} \end{aligned} \tag{10}$$

$$P_{Iso} \coloneqq \{\vec{u} \in \Re^m | \vec{u} = \mathcal{P}_{\mathcal{N}(B)}\vec{u}', \vec{u}' \in \Omega\} \tag{11}$$

Equation 10 shows that the MP surface (P_{Smin}) can be visualized as the AMS (Φ) mapped by P_{min} to the control space or equivalently as the orthogonal projection of the Allowable Control Set onto the subspace formed by the span of MP generalized inverse matrix (P_{min}) column vectors. It is important to note that the MP surface is not entirely contained within the ACS (i.e. $P_{Smin} \not\subset \Omega$). Lastly, it is assumed in this paper that the controls effectiveness matrix B consists of non-coplanar controls or equivalently that B is of robust rank. Durham [1, 8] defines robust rank for $B \in \Re^{n\times m}$ as every $n \times n$ combination of B is of full rank.

1. Moore-Penrose Control Allocation Problem Basis Vector Selection

The inherent decomposition of the control vector $\vec{u}$ described previously motivates the selection of an orthogonal basis vector set $\hat{\mathcal{B}}$ for expressing $\vec{u}$ that in the sequel is shown to facilitate solving the MP controls allocation problem over the entire Attainable Moment Set. This $\hat{\mathcal{B}}$ set consists of one vector $\hat{u}_{des} \in P_{Smin}$ and the complete set of P_{Iso} basis vectors $\hat{B} \coloneqq \begin{bmatrix}\hat{b}_1 & \hat{b}_2 & \dots & \hat{b}_{m-n}\end{bmatrix}$. Given a desired-moment $\vec{m}_{des} \in \Phi$, we define $\vec{u}_{des}$ the control subspace companion vector to $\vec{m}_{des}$ as:

$$\vec{u}_{des} = P_{min}\vec{m}_{des} \tag{12}$$

From equation (12) we define the basis vector $\hat{u}_{des}$ as:

$$\hat{u}_{des} \coloneqq \frac{\vec{u}_{des}}{\|\vec{u}_{des}\|_2} \tag{13}$$

Equations (13) and (11) concatenated complete the basis $\hat{\mathcal{B}}$ with orthogonal unit vector columns:

$$\hat{\mathcal{B}} \coloneqq \begin{bmatrix}\hat{u}_{des} & \hat{b}_1 & \hat{b}_2 & \dots & \hat{b}_{m-n}\end{bmatrix} \tag{14}$$

Now the basis vector matrix $\hat{\mathcal{B}}$ can be used to express an arbitrary $\vec{u}$ (for a given $\vec{m}_{des}$) as:

$$\begin{aligned} &\vec{u} \coloneqq \hat{\mathcal{B}}_v\vec{g} = \begin{bmatrix}\hat{u}_{des} & \hat{b}_1 & \hat{b}_2 & \dots & \hat{b}_{m-n}\end{bmatrix}\vec{g} \text{ with } \vec{g} \coloneqq \begin{bmatrix}a & b_1 & b_2 & \dots & b_{m-n}\end{bmatrix}^T \\ &\text{where } a, b_i \in \Re \end{aligned} \tag{15}$$

Equations 7 and 15 show $\vec{u}$ can be decomposed as:

$$\vec{u}_{\|} = a\hat{u}_{des} \tag{16}$$

$$\vec{u}_{\perp} = \begin{bmatrix}\hat{b}_1 & \hat{b}_2 & \dots & \hat{b}_{m-n}\end{bmatrix}\begin{bmatrix}b_1 & b_2 & \dots & b_{m-n}\end{bmatrix}^T \tag{17}$$

The decomposed components of $\vec{u}$ are graphically depicted in Fig. (1) along with the appropriate transformation matrices to map these components between the relevant subsets.

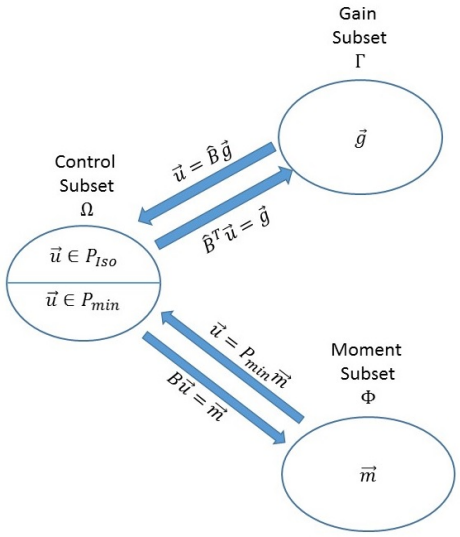

Fig. 1 Graphic Depiction of Transformations Between Subsets

2. Subsets of Allowable Control Set and Attainable Moment Set

In order to understand the limitations of the MP generalized inverse, Fig. 2 depicts the divisions in Ω and Φ based on the generalized inverse P_{min} and the associated MP surface P_{Smin}. The divisions of Ω are:

$$\Omega_1 \coloneqq \{\vec{u} \in \Omega \cap P_{Smin}\} \tag{18}$$

$$\Omega_2 \coloneqq \{\vec{u} \in \Omega | \mathcal{P}_{P_{min}}\vec{u} \in \Omega \cap P_{Smin}\} \tag{19}$$

$$\Omega_3 \coloneqq \{\vec{u} \in \Omega_4 | \forall \vec{u}' \in \Omega_4 \text{ where } \mathcal{P}_{P_{min}}\vec{u} = \mathcal{P}_{P_{min}}\vec{u}', \|\vec{u}\|_2 < \|\vec{u}'\|_2\} \tag{20}$$

$$\Omega_4 \coloneqq \{\vec{u} \in \Omega | \mathcal{P}_{P_{min}}\vec{u} \in \Omega^C \cap P_{Smin}\}, \text{ where } \Omega^C \coloneqq \Re^m \setminus \Omega \tag{21}$$

and similarly the Attainable Moment Set Φ is divided into two subsets as follows:

$$\Phi_1 \coloneqq \{\vec{m} \in \Phi | \vec{u} \in \Omega_1, B\vec{u} = \vec{m}\} \tag{22}$$

$$\Phi_3 \coloneqq \{\vec{m} \in \Phi | \vec{u} \in \Omega_3, B\vec{u} = \vec{m}\} \tag{23}$$

Some important relationships among the above subsets are:

$$\Omega_1 \subset \Omega_2 \tag{24}$$

$$\Omega_3 \subset \Omega_4 \tag{25}$$

$$\Omega_2 \cup \Omega_4 = \Omega \text{ and } \Omega_2 \cap \Omega_4 = \emptyset \tag{26}$$

$$\forall \vec{m} \in \Phi \implies BP_{min}\vec{m} = \vec{m} \in \Re^n \tag{27}$$

$$\forall \vec{u} \in \Omega_1 \quad P_{min}B\vec{u} = \vec{u} \in \Re^m \tag{28}$$

$$\Phi_1 \cup \Phi_3 = \Phi \text{ and } \Phi_1 \cap \Phi_3 = \emptyset \tag{29}$$

The above relationships between the respective subsets are proven in Appendix B.

Some comments on the significance of these Ω and Φ subsets follow. For the rectilinearly constrained case, Φ_1 represents the well known region in literature for which the Moore-Penrose generalized inverse matrix solves the control allocation problem without exceeding any control position constraints. Equations (27,28) demonstrate the one-to-one and onto (i.e. homeomorphism) relationship between the compact sets Ω_1 and Φ_1. Since Ω_1 is the P_{min}-mapping of Φ_1 to control space, and Φ_1 is the region for which the MP generalized inverse provides unique minimum 2-norm solutions, then Ω_1 is the complete set of MP optimal control allocation solutions that are MP achievable using P_{min} without violating any control constraints. Conversely, Ω_2 is the complete set of all control solutions (MP optimal and non-optimal) for which the controls effectiveness matrix B maps to Φ_1. Specifically, for each moment in Φ_1, Ω_1 contains the unique (achievable) MP optimal control allocation solution while Ω_2 contains this same optimal solution and all

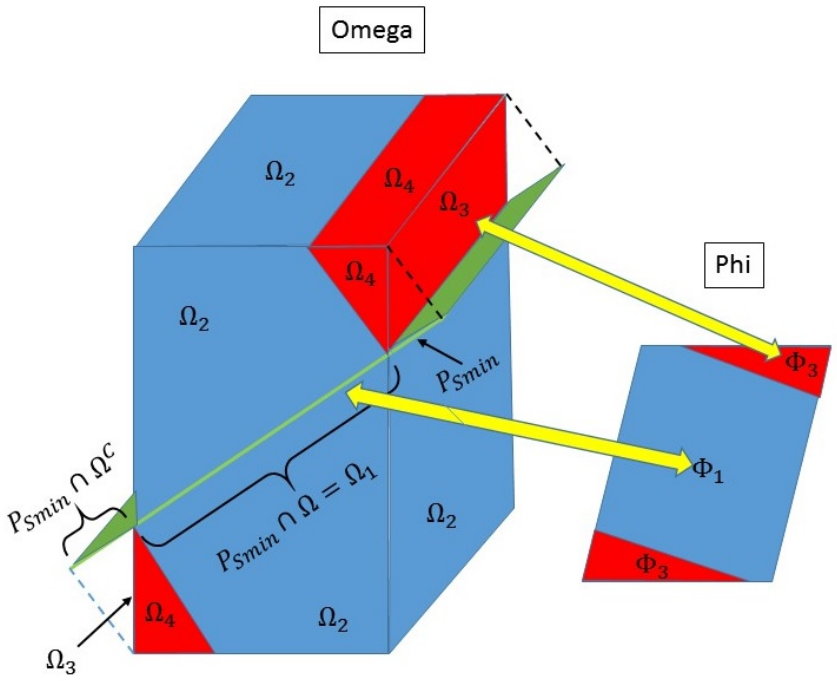

Fig. 2 Graphic Depiction of Control and Moment Subsets

other possible control solutions using the $\mathcal{N}(B)$ that yield the specific moment in Φ_1 without violating any control constraints.

The subset Φ_3 is the region for which the Moore-Penrose generalized inverse matrix fails to provide MP control allocation solutions without violating control constraints. Durham [1] noted that there does not exist any choice of generalized inverse matrix that covers the entire AMS. Thus there is no generalized inverse for which $\Phi_3 = \emptyset$ or equivalently for which $\Phi_1 = \Phi$. The research in this paper, shows both the existence and uniqueness of MP optimal control allocation solutions $\vec{u}_{opt} \in \Omega_3, \forall \vec{m} \in \Phi_3$ and an analytical online method to compute them. It should be noted that Ω_4 contains all control solutions (MP optimal and non-optimal) that map to Φ_3, while Ω_3 contains only the MP optimal control allocation solutions that map to Φ_3. Lastly, it is important to note that the definition of Ω_3 provides insight that all MP optimal control allocation solutions for $\vec{m} \in \Phi_3$ are contained on a specific subset of $\delta(\Omega)$ (i.e. the ones 2-norm nearest to P_{Smin}).

B. Existence and Construction of Unique MP Optimal Control Allocation Solutions

A main goal of this paper is to first prove the existence of a unique minimum 2-norm control $\vec{u}_{opt} \in \Omega$ with rectilinear control position constraints for each $\vec{m}_{des} \in \Phi$ and then to introduce the Prediction Method as an algorithm to construct these MP optimal allocation solutions $\vec{u}_{opt}, \forall \vec{m}_{des} \in \Phi$. The existence of MP optimal allocation solutions is proven in Appendix A. The Prediction Method is introduced by first using a numerical example to highlight the trend that MP optimal control allocation solutions along a fixed moment direction are piecewise linear and continuous. This observed trend is the basis for the Prediction Method which analytically solves for the end points along each linear segment of the MP optimal allocation solutions. Once the Prediction Method solutions are delineated, they are shown equivalent to be MP optimal control allocation solutions under the assumption that the nearest Allowable Control Set boundary is known.

The existence is proven in two parts for the subsets Ω_1 and Ω_3 depicted in the Fig. 2. First, the MP optimal solutions for $\vec{m}_{des} \in \Phi_1$ correspond with $\vec{u}_{opt} \in \Omega_1$ and are equivalent to the unconstrained case proven in Theorem 1 of Appendix A. The unconstrained optimal solutions are $\vec{u}_{opt} = \vec{u}_{des} := P_{min}\vec{m}_{des}$ (which is a well known result) and thus we not only have existence but a method to compute them. Conversely, the MP optimal solutions for $\vec{m}_{des} \in \Phi_3$ correspond with $\vec{u}_{opt} \in \Omega_3$ and are equivalent to the constrained case proven in Theorem 2. The solution for the constrained control case is of the form $\vec{u}_{opt} = \vec{u}_{des} + \vec{u}_{\perp min}$ where $\vec{u}_{\perp min} \in P_{Iso}$ and $\vec{u}_{\perp min}$ is the unique minimum

vector required such that $\vec{u}_{opt} \in \delta(\Omega)$. So while Theorem 2 proves the existence of the MP optimal control solutions, the subsequent material will show the Prediction Method is an iterative algorithm to compute them.

1. Observation of Continuous Piecewise Linearity of Optimal Allocation Solutions Along Desired Moment Direction

In a typical Moore-Penrose optimal control algorithm implementation, the objective is to determine the unique minimum 2-norm control allocation solution $\vec{u}_{opt}$ (if it exists) for a specific desired moment $\vec{m}_{des}$. While typical implementations (e.g. Interior Point Algorithm) may seek a single solution for a given moment, there is utility in examining the complete family of MP optimal control allocation solutions in a fixed moment direction $\hat{m}_{des}$ from the origin to $\delta(\Phi)$. Given a fixed $\vec{m}_{des}$, we define the desired moment unit vector as:

$$\hat{m}_{des} \coloneqq \frac{\vec{m}_{des}}{\|\vec{m}_{des}\|_2} \tag{30}$$

A numerical example taken from literature [2] is shown below which consists of the controls effectiveness matrix (B) and control position constraints ($\vec{u}_{upr}$ and $\vec{u}_{lwr}$):

$$B = \tag{31}$$
$$\begin{bmatrix} -4.38e^{-2} & 4.38e^{-2} & -5.84e^{-2} & 5.84e^{-2} & 1.67e^{-2} & -6.28e^{-2} & 6.28e^{-2} & 2.92e^{-2} & 1e^{-5} & 1.0e^{-2} \\ -53.3e^{-2} & -53.3e^{-2} & -6.49e^{-2} & -6.49e^{-2} & 0 & 6.23e^{-2} & 6.23e^{-2} & 1e^{-5} & 35.53e^{-2} & 1e^{-5} \\ 1.1e^{-2} & -1.1e^{-2} & 3.91e^{-2} & -3.91e^{-2} & -7.43e^{-2} & 0 & 0 & 3e^{-4} & 1e^{-5} & 14.85e^{-2} \end{bmatrix}$$

$$\vec{u}_{upr} = \begin{bmatrix} 0.183 & 0.183 & 0.524 & 0.524 & 0.524 & 0.785 & 0.785 & 0.524 & 0.524 & 0.524 \end{bmatrix}^T \tag{32}$$

$$\vec{u}_{lwr} = \begin{bmatrix} -0.419 & -0.419 & -0.524 & -0.524 & -0.524 & -0.140 & -0.140 & -0.524 & -0.524 & -0.524 \end{bmatrix}^T \tag{33}$$

For the numerical example shown in subsequent Figs. 3-4, an arbitrary $\vec{u}$ was chosen as on $\delta(\Omega)$ such that $B\vec{u} \in \delta(\Phi)$. The particular choice of $\vec{u}$ was:

$$\vec{u} = \begin{bmatrix} -0.419 & -0.419 & -0.524 & -0.524 & -0.524 & -0.14 & 0.785 & 0.524 & 0.524 & 0.524 \end{bmatrix}^T \tag{34}$$

which consisted of one of 2^{10} permutations for which all control effectors were saturated at either their respective lower or upper position limits. The corresponding moment vector ($\vec{m}_{des} = B\vec{u}$) was used to create a set of monotonically increasing 2-norm magnitude moment vectors in the direction of $\hat{m}_{des}$ according to:

$$M \coloneqq \{\vec{m}_{des_0}, \vec{m}_{des_1}, \ldots, \vec{m}_{des_{100}}\} \text{ where } \vec{m}_{des_i} \coloneqq \frac{i}{100} \times \|\vec{m}_{des}\|_2 \, \hat{m}_{des} \text{ with } i \in \{0, 1, \ldots 100\} \tag{35}$$

Next, the Matlab constrained non-linear solver fmincon (interior point) was used to find 2-norm minimal solutions $\vec{u}_i$ for each $\vec{m}_i \in M$ such that $B\vec{u}_i = \vec{m}_i$ and $\vec{u}_{lwr} \leq \vec{u}_i \leq \vec{u}_{upr}$ element wise yielding the MP optimal control allocation solution set:

$$U \coloneqq \{\vec{u}_{opt_0}, \vec{u}_{opt_1}, \ldots, \vec{u}_{opt_{100}}\} \tag{36}$$

Now utilizing the $\hat{\mathcal{B}}$ basis matrix defined in equation (14) it is straightforward to express the obtained family of MP optimal control solutions in terms of the selected basis vector gains. In particular, since the columns of $\hat{\mathcal{B}}$ consists of orthogonal unit vectors multiplication of equation (15) by $\hat{\mathcal{B}}^T$ implies:

$$\vec{g}_{opt_i} = \hat{\mathcal{B}}^T \vec{u}_{opt_i} \text{ where } \vec{g}_{opt_i} \in \mathfrak{R}^{m-n+1} \tag{37}$$

Fig. 3 plots the progression of control effector saturation which occurs as a function of $\left\|\vec{m}_{des_i}\right\|_2$. The results for both $\vec{g}_{opt_i}$ and $\vec{u}_{opt_i}$ are shown in Figs. (4-5). Specifically, Figs. 4 and 5 plot selected basis gains and control effector position (respectively) as a function of $\left\|\vec{m}_{des_i}\right\|_2$. Fig. 3 is representative of the trends observed with a wide array of various linear control effector matrices with robust rank. Specifically, the initial control effector saturation occurs at the intersection of the $\hat{u}_{des}$ vector extended with increasing a_0 gain in P_{Smin} until it intersects with $\delta(\Omega)$. As the a_0 gain

is increased further, additional control effectors are saturated and gains b_1 to b_{m-n} are required to return the control effectors within the ACS.

Figs. 4 & 5 clearly demonstrate the piecewise linear and continuous nature of both the basis gains and the associated control effector positions as a function of increasing $\|\vec{m}_{des}\|_2$. The PM algorithm makes use of the linearity to iteratively solve for each linear solution segment along a fixed $\hat{m}_{des}$.

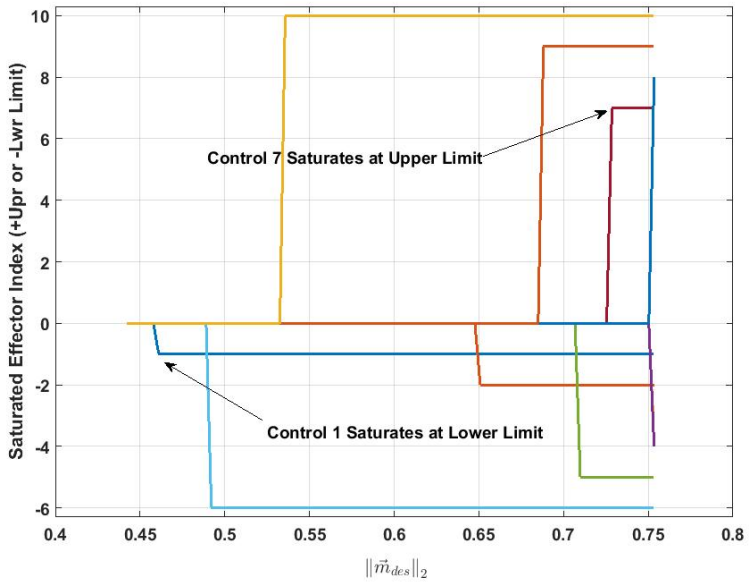

Fig. 3 Progression of Control Saturation versus $\|\vec{m}_{des}\|_2$

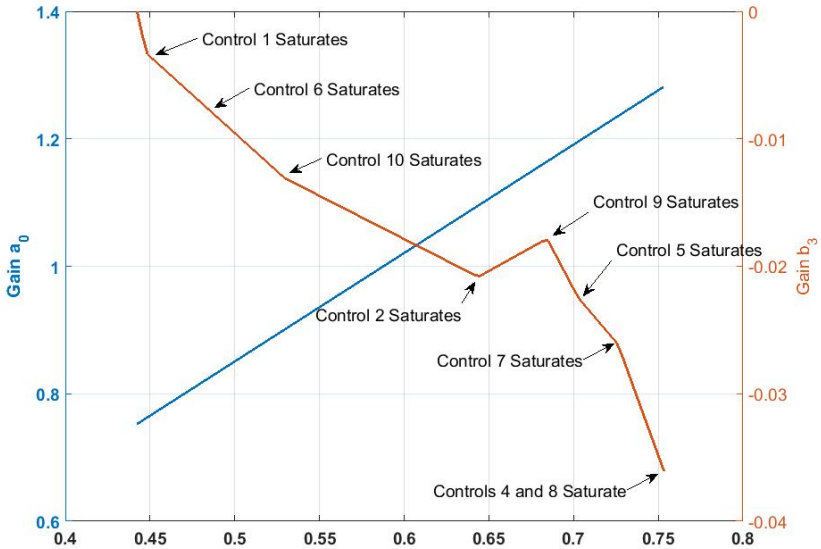

Fig. 4 Basis Gain versus $\|\vec{m}_{des}\|_2$

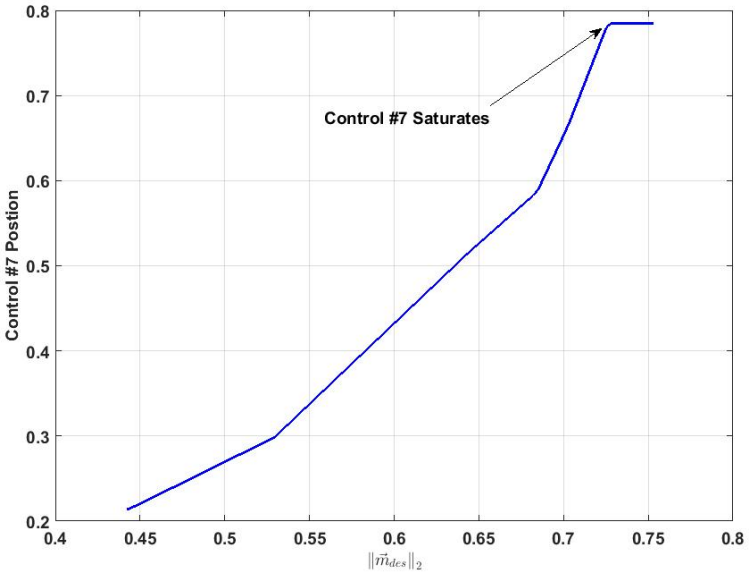

Fig. 5 Control Position versus $\|\vec{m}_{des}\|_2$

C. Construction of Optimal Control Allocation Solutions Using the Prediction Method Iterative Algorithm

In light of the aforementioned choice to express controls allocation solutions using the selected basis vectors and associated gains, typical optimizers could be viewed as tackling the MP controls allocation problem by simultaneously finding the $\hat{u}_{des}$ basis vector gain (a) and the null space basis vector gains ($\vec{b}$) that achieves $\vec{u}_{opt}$ which in turn yields the desired $\vec{m}_{des}$ while maintaining the controls within position limits. The prediction method algorithm takes advantage of the piece-wise linear and continuous nature of the MP control allocation solutions to separate the determination of the a gain from the $\vec{b}$ gains. This simplification allows for direct analytic solutions which successively solve for a then $\vec{b}$ then a etc.. As seen in Fig. 4, the $\hat{B}$ gain lines change direction as each successive new control effector is saturated. In this paper, the region on the $\delta(\Omega)$ at which a new control effector saturation occurs or equivalently at which the null space gains change direction is referred to as a "corner". The prediction method, finds the a^* and $\vec{b}^*$ gains at each corner and stores these as well as the associated 2-norm of each respective corner moment. The resulting table is then used to determine with very high precision the MP optimal control solution for any desired moment for a given (fixed) $\hat{m}_{des}$.

In overview, the prediction algorithm process proceeds as follows: Determination of the first corner is performed by finding the $\hat{u}_{des}$ gain a such that $a\hat{u}_{des} \cap \delta(\Omega)$ saturates the first control effector. At this corner, the only gain is a (i.e. $\vec{b} = \vec{0}$). This first corner's gains and the 2-norm of the current solution generated moment is stored. For all subsequent corners, small steps are taken in a (e.g. $a + \Delta a$), and then a local optimization problem is analytically solved to determine the "slope" of the change in optimal controls per unit gain $\frac{\Delta\vec{u}_{opt}}{\Delta a}$. This control slope is used in one-step to determine the next control effector that will be saturated and to generate the a^* gain associated with the next corner. Once the correct a^* gain at the successive corner is known then the local optimization problem is repeated using the new fixed a^* to determine $\vec{b}^*$ at the corner. These corner gain results, a^* and $\vec{b}^*$ and the 2-norm of this corner's resulting moment are stored. The process is repeated for successive corners, until m-n controls are saturated (or in some cases all controls are saturated) and/or any further increase in a gain prevents any null space vector from returning the control allocation solution to $\delta(\Omega)$.

After the iterative algorithm has run from the origin to the boundary of the AMS, a corner lookup table has been generated for all possible MP optimal control allocation solutions along a desired moment direction $\hat{m}_{des}$ from the origin to $\delta(\Phi)$. Linear regression is then performed on this table to "predict" the exact basis vector gains (a and $\vec{b}$) for any given $\vec{m}_{des} \in [0, \vec{m}_{max}]$ in the direction of $\hat{m}_{des}$. Using these predicted gains then MP optimal control allocation solution is found as: $\vec{u}_{opt} = \hat{\mathcal{B}} \begin{bmatrix} a_{pred} & \vec{b}_{pred}^T \end{bmatrix}^T$.

1. Local Optimization to Return Control Vector to Allowable Control Set

This section defines a localized cost function and analytically solves for a proven 2-norm minimal null space vector which returns the total control solution to the Allowable Control Set for a fixed $\hat{u}$ gain (a).

Noting that the first control effector is saturated (i.e. first corner) when the $\hat{u}_{des}$ gain a satisfies:

$$\vec{u}_{opt} = \vec{u}_{\parallel} = a\hat{u}_{des} \cap \delta(\Omega) \in P_{Smin} \text{ with } \vec{u}_{\perp} = 0 \tag{38}$$

As we need to maintain an updated list of saturated and unsaturated effectors we define the following notation:

$$S_2 \coloneqq \{\text{Saturated Control Effector Indices}\} \tag{39}$$

$$\vec{s}_2 \coloneqq \{\text{Column Vector of Saturated Control Effector Limits (Upper or Lwr)}\} \tag{40}$$

$$S_1 \coloneqq \{\text{Unsaturated Control Effector Indices}\} = \{1, 2, \ldots, m\} \setminus S_2 \tag{41}$$

We know that for any $\hat{u}_{des}$ gain a greater than that which satisfies Eq. 38, $\vec{u}_{\perp}$ is required to return $\vec{u} \in \Omega$. This section formulates and solves a local optimization problem which analytically solves for $\vec{u}_{\perp} = \hat{B}\vec{b}$ with the smallest 2-norm such that $a\hat{u}_{des} + \vec{u}_{\perp} \in \delta(\Omega)$. Since $a\hat{u}_{des}$ completely prescribes the resulting moment ($aB\hat{u}_{des} = \vec{m}$) and for a given $\vec{m}$ the value of a is unique, therefore $a\hat{u}_{des}$ is the exact component of $\vec{u} \in P_{Smin}$ required to achieve $\vec{m}$. As shown in Theorem (2), the vector $\vec{u}_{des} \notin \Omega$ requires finding the 2-norm shortest vector $\vec{v} \in P_{iso}$ to return $\vec{u}_{des} + \vec{v} \in \delta(\Omega)$. This section solves a local optimization problem with equality constraints using a Lagrange multiplier to determine the $\vec{v} \in P_{iso}$ with the smallest 2-norm.

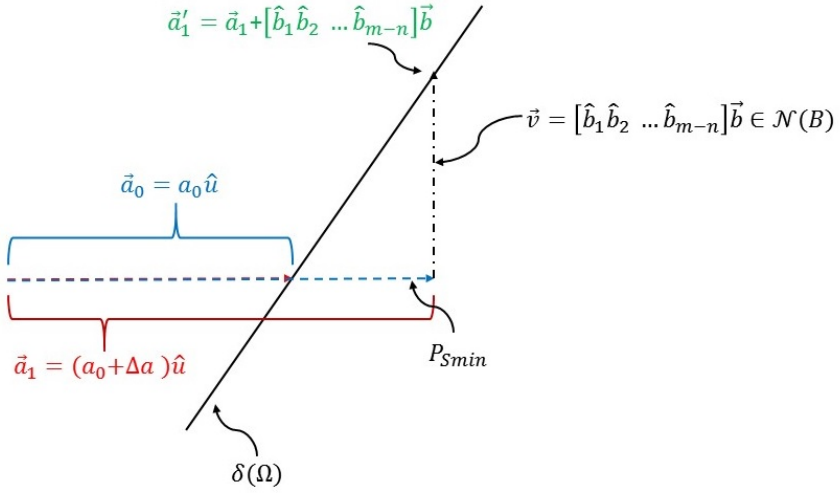

Fig. 6 Local Optimization Return to Boundary of Allowable Control Set

Graphically, for any given "corner" specified by a particular $\vec{a}_0$ or equivalently by the scalar a_0 we have $\vec{a}_0 = a_0\hat{u}_{des}$, then the components of $\vec{a}_0$ corresponding to saturated controls are on $\delta(\Omega)$. Next a small step in a_0 gain is taken yielding the new vector $\vec{a}_1 \coloneqq (a_0 + \Delta a)\,\hat{u}_{des}$. The small Δa gain step drives all saturated components off the boundary and yields $\vec{a}_1$ off the $\delta(\Omega)$. The problem is to find the optimal (minimal 2-norm) vector $\vec{v}$ to return only the saturated components of the vector $\vec{a}_1' \coloneqq (a_0 + \Delta a)\,\hat{u} + \left[\hat{b}_1 \quad \hat{b}_2 \quad \ldots \quad \hat{b}_{m-n}\right]\vec{b}$ back to $\delta(\Omega)$. Figure (6) shows that the saturated components of $\vec{a}_0$ and $\vec{a}_1'$ on $\delta(\Omega)$ are identical which suggests defining a local optimization cost function with equality constraints as:

$$J\left(\vec{b}, \vec{\lambda}\right) \coloneqq \frac{1}{2}\vec{b}^T \left[\hat{b}_1 \quad \hat{b}_2 \quad \ldots \quad \hat{b}_{m-n}\right]^T \left[\hat{b}_1 \quad \hat{b}_2 \quad \ldots \quad \hat{b}_{m-n}\right]\vec{b} + \vec{\lambda}^T\left(\vec{a}_{0sat} - \vec{a}_{1sat} - \left[\hat{b}_{1sat} \quad \hat{b}_{2sat} \quad \ldots \quad \hat{b}_{(m-n)sat}\right]\vec{b}\right)$$

where the subscript "sat" refers to utilizing only the row components of the respective vector/matrix that correspond to the current list of saturated controls (S_2). But since $\hat{B}$ has columns that are orthogonal unit vectors, then

$\left[\hat{b}_1 \quad \hat{b}_2 \quad \dots \quad \hat{b}_{m-n}\right]^T \left[\hat{b}_1 \quad \hat{b}_2 \quad \dots \quad \hat{b}_{m-n}\right] = \hat{B}^T\hat{B} = I$ which yields:

$$J\left(\vec{b},\vec{\lambda}\right) \coloneqq \frac{1}{2}\vec{b}^T\vec{b} + \vec{\lambda}^T\left(\vec{a}_{0sat} - \vec{a}_{1sat} - \hat{B}_{sat}\vec{b}\right) \tag{42}$$

Appendix C shows and analyzes the first order necessary and second order sufficient conditions of Eq. (42) and derives the minimal solution as (see Eq. 121):

$$\vec{b}_{min} = \hat{B}_{sat}^T\left(\hat{B}_{sat}\hat{B}_{sat}^T\right)^{-1}\left(\vec{a}_{0sat} - \vec{a}_{1sat}\right) \tag{43}$$

Thus given $\vec{b}_{min}$ then:

$$\vec{u}_{opt} = \begin{bmatrix}\hat{u} & \hat{b}_1 & \hat{b}_2 & \dots & \hat{b}_{m-n}\end{bmatrix}\begin{bmatrix}a_0 \\ \vec{b}_{min}\end{bmatrix} \tag{44}$$

$$\tag{45}$$

It is important to note that there is an inherent assumption here on having the "correct" list of currently saturated controls or equivalently knowing which is the nearest portion of the $\delta(\Omega)$. If the correct list of saturated controls is known, then the minimal null space gains which get the solution to the nearest $\delta(\Omega)$ not only return the saturated controls to $\delta(\Omega)$ but also yield non-saturated controls that are within control position limits or:

$$\vec{u}_{opt_i} \in \delta(\Omega)\,\forall i \in S_2 \text{ and } \vec{u}_{lwr} \le \vec{u}_{opt_i} \le \vec{u}_{upr}\forall i \in S_1 \tag{46}$$

While it is intuitive that if you return to the boundary of Ω then all control effectors are within Ω limits, it has also been shown heuristically in numerical analysis. Conversely, for a given $\vec{b}_{min}$, if the resulting non-saturated controls (see Eq. 46) are not within control position limits then this shows that the current list of saturated controls is incorrectly specifying the nearest portion of $\delta(\Omega)$.

2. Control Direction Unit Vector Gain Update and Determination of Next Saturated Control Effector

The previous section derived an analytic local optimization problem which was shown to find the minimal basis vector gains that correspond with a small step in a_0. Since these optimal basis gains are piecewise linear and continuous, then knowledge of the corner point and any one point along the optimal basis vector gain lines is sufficient to have knowledge of all points along a particular piecewise linear line segment. The prediction method algorithm makes use of the current corner point and two points along the optimal basis vector gain lines to solve for the next saturated control. These two additional points provide a very precise calculation of "slope" which increases numerical accuracy and typically finds the next corner in one step with near machine precision. The process of locating the next corner starts with defining two vectors ($\vec{a}_1$ and $\vec{a}_2$) where:

$$\vec{a}_1 \coloneqq (a_0 + \Delta a)\,\hat{u}_{des} \qquad \vec{a}_2 \coloneqq (a_0 + 2\Delta a)\,\hat{u}_{des} \tag{47}$$

Now the local optimization (equation 43) is solved for both $\vec{a}_1$ and $\vec{a}_2$ yielding $\vec{b}_{1_{min}}$ and $\vec{b}_{2_{min}}$. These minimal basis gains are then used to compute two MP optimal control points:

$$\vec{a}'_1 \coloneqq \hat{\mathcal{B}}\begin{bmatrix}(a_0 + \Delta a) \\ \vec{b}_{1_{min}}\end{bmatrix} \tag{48}$$

$$\vec{a}'_2 \coloneqq \hat{\mathcal{B}}\begin{bmatrix}(a_0 + 2\Delta a) \\ \vec{b}_{2_{min}}\end{bmatrix} \tag{49}$$

Next defining the rate of change of optimal control solutions per unit change in gain a_0, we have:

$$\Delta\vec{u}_{opt_i} \coloneqq \frac{\vec{a}'_{2_i} - \vec{a}'_{1_i}}{\Delta a} \qquad \forall i \in S_1 \tag{50}$$

The "direction" of the change in optimal control solutions is used to determine whether each unsaturated control is proceeding towards the upper or lower respective limit.

$$\forall i \in S_1, \qquad \vec{u}_{lim_i} \coloneqq \begin{cases} \text{sgn}\left(\vec{a}'_{2_i} - \vec{a}'_{1_i}\right) > 0, & \vec{u}_{upr_i} \\ \text{sgn}\left(\vec{a}'_{2_i} - \vec{a}'_{1_i}\right) = 0, & \text{N/A} \\ \text{sgn}\left(\vec{a}'_{2_i} - \vec{a}'_{1_i}\right) < 0, & \vec{u}_{lwr_i} \end{cases} \tag{51}$$

Then using equations (50 and 51), we can solve for the change in gain a_0 required to saturate control $\vec{u}_i$ using:

$$\delta a_{0_i} \coloneqq \frac{\left|\vec{u}_{lim_i} - \vec{a}'_{1_i}\right|}{\Delta \vec{u}_{opt_i}} \qquad \forall i \in S_1 \tag{52}$$

Now we use the minimum δa_{0_i} to determine the a_1^* gain at the next corner:

$$a_1^* = a_0 + \Delta a + \min_{\delta a_0}\{\delta a_{0_i} | \forall i \in S_1\} \tag{53}$$

Note that the control effector index $i \in S_1$ which yields the minimum δa_{0_i} determines which control will be added to the set of saturated controls (S_2) during the next corner iteration. Finally, solving for the minimal null space basis gains ($\vec{b}^*_{min}$) at the upcoming corner yields the optimal controls at that corner and $\vec{u}^*_{opt}$ is found using:

$$\vec{a}_0 = a_0\hat{u}, \quad \vec{a}_1^* = a_1^*\hat{u} \implies \tag{54}$$

$$\vec{b}^*_{min} = \hat{B}^T_{sat}\left(\hat{B}_{sat}\hat{B}^T_{sat}\right)^{-1}\left(\vec{a}_{0sat} - \vec{a}^*_{1sat}\right) \implies \tag{55}$$

$$\vec{u}^*_{opt} = \hat{\mathcal{B}}\begin{bmatrix} a_1^* \\ \vec{b}^*_{min} \end{bmatrix} \tag{56}$$

The values for a_1^*, $\vec{b}^*_{min}$ and $\|\vec{m}^*\|_2 = \left\|B\vec{u}^*_{opt}\right\|_2$ are stored for the current corner. The sets S_1, S_2, and the vector $\vec{s}_2$ are all updated and the process is repeated for each corner until any further increase in a_0 prevents a solution which is on $\delta(\Omega)$. Note that the original corner location $\vec{a}_0$ has saturated components $\vec{s}_2$ from the saturated component indices set S_2 and therefore $\vec{a}_{0_{sat}} = \vec{s}_2$. Thus Eq. (55) is equivalent to:

$$\vec{b}^*_{min} = \hat{B}^T_{sat}\left(\hat{B}_{sat}\hat{B}^T_{sat}\right)^{-1}\left(\vec{s}_2 - \vec{a}^*_{1sat}\right) \tag{57}$$

The total optimal control allocation solution can then be expressed as:

$$\vec{u}^*_{opt} = \vec{c}_0^* + \vec{c}_1^* + a_1^*\hat{u}_{des}, \text{ where} \tag{58}$$

$$\vec{c}_0^* \coloneqq \hat{B}^T_{sat}\left(\hat{B}_{sat}\hat{B}^T_{sat}\right)^{-1}\vec{s}_2, \quad \vec{c}_0^* \in P_{Iso} \tag{59}$$

$$\vec{c}_1^* \coloneqq -\hat{B}^T_{sat}\left(\hat{B}_{sat}\hat{B}^T_{sat}\right)^{-1}\vec{a}^*_{1sat}, \quad \vec{c}_1^* \in P_{Iso} \tag{60}$$

Additionally, since $a_1^*\hat{u}_{des} \in P_{Smin}$, then by Eqs. (18,28) we have $\vec{m}^*_{des} = B\left(a_1^*\hat{u}_{des}\right) \implies P_{min}\vec{m}^*_{des} = a_1^*\hat{u}_{des}$ and therefore:

$$\vec{u}^*_{opt} = \vec{c}_0^* + \vec{c}_1^* + P_{min}\vec{m}^*_{des}, \text{ where} \tag{61}$$

$$\vec{c}_0^* \coloneqq \hat{B}^T_{sat}\left(\hat{B}_{sat}\hat{B}^T_{sat}\right)^{-1}\vec{s}_2 \tag{62}$$

$$\vec{c}_1^* \coloneqq -\hat{B}^T_{sat}\left(\hat{B}_{sat}\hat{B}^T_{sat}\right)^{-1}\left(P_{min}\vec{m}^*_{des}\right)_{sat} \tag{63}$$

3. Table Lookup: Basis Gain Prediction for Given Desired Moment

This section demonstrates how to use the stored MP optimal basis gain vectors and the associated 2-norm corner moments to predict the basis gains for any desired moment along $\hat{m}_{des}$. Let $\vec{g}_i^* \coloneqq \begin{bmatrix} a^* & b_1^* & b_2^* & \dots & b_{m-n}^* \end{bmatrix}^T$ be the optimal gain vector for the i-th corner. Additionally, for each corner the 2-norm of moment $\left\|\vec{m}_i^*\right\|_2$ is given. Then the optimal gain vectors for each corner are concatenated in matrix form:

$$G^* \coloneqq \begin{bmatrix} \vec{g}_1^{*T} \\ \vec{g}_2^{*T} \\ \vdots \\ \vec{g}_k^{*T} \end{bmatrix}, \text{ where } G^* \in \Re^{k\times(m-n+1)} \text{ with k = number of corners} \tag{64}$$

The 2-norm moments are similarly concatenated:

$$M^* = \begin{bmatrix} 1 & \left\|\vec{m}_1^*\right\|_2 \\ 1 & \left\|\vec{m}_2^*\right\|_2 \\ \vdots & \vdots \\ 1 & \left\|\vec{m}_k^*\right\|_2 \end{bmatrix} \tag{65}$$

Now for a given $\vec{m}'$ such that $\vec{m}' \parallel \hat{m}_{des}$ we wish to use equations (64,65) to determine $\vec{u}'_{pred}$. The solution falls into three categories (with k = # of corners):

1) $\|\vec{m}'\|_2 \le \left\|\vec{m}_1^*\right\|_2$
2) $\left\|\vec{m}_1^*\right\|_2 \le \|\vec{m}'\|_2 \le \left\|\vec{m}_k^*\right\|_2$
3) $\left\|\vec{m}_k^*\right\|_2 < \|\vec{m}'\|_2$

Cases 1 and 3 are straightforward. For case 1: $\vec{g}_{pred} = \vec{g}_1^* \frac{\|\vec{m}'\|_2}{\left\|\vec{m}_1^*\right\|_2}$ where $\vec{g}_1^* = \begin{bmatrix} a_1^* \\ \vec{0}_1 \end{bmatrix}$ so then:

$$\vec{u}'_{pred} = a_1^* \frac{\|\vec{m}'\|_2}{\left\|\vec{m}_1^*\right\|_2}\hat{u} = \hat{\mathcal{B}}\vec{g}_1^* \frac{\|\vec{m}'\|_2}{\left\|\vec{m}_1^*\right\|_2} \tag{66}$$

For case 3 where the desired moment exceeds the maximum moment on the $\delta(\Phi)$ then the best MP optimal control solution available is the maximum moment on the $\delta(\Phi)$. Therefore $\vec{g}_{pred} = \vec{g}_k^{*T}$ so then:

$$\vec{u}'_{pred} = \vec{u}^*_{pred} = \hat{\mathcal{B}}\vec{g}_k^{*T} \tag{67}$$

Case 2 requires a piece-wise linear regression by first determining the i index:

$$i \in \{1, 2, \dots, k-1\} \text{ such that } \left\|\vec{m}_i^*\right\|_2 \le \|\vec{m}'\|_2 \le \left\|\vec{m}_{i+1}^*\right\|_2 \tag{68}$$

and then setting up the normal equation:

$$G = MC \implies C = \left(M^T M\right)^{-1} M^T G \text{ where } G = \begin{bmatrix} \vec{g}_i^{*T} \\ \vec{g}_{i+1}^{*T} \end{bmatrix} \text{ and } M = \begin{bmatrix} 1 & \left\|\vec{m}_i^*\right\|_2 \\ 1 & \left\|\vec{m}_{i+1}^*\right\|_2 \end{bmatrix} \tag{69}$$

where C is of the form:

$$C = \begin{bmatrix} C_{01} & C_{02} & \dots & C_{0(m-n)+1} \\ C_{11} & C_{12} & \dots & C_{1(m-n)+1} \end{bmatrix} \tag{70}$$

and the rows of C are the regression intercept and slope gain vectors respectively. So then $\vec{u}'_{pred}$ is:

$$\vec{u}'_{pred} = \hat{\mathcal{B}}C^T \begin{bmatrix} 1 \\ \|\vec{m}'\|_2 \end{bmatrix} \tag{71}$$

Note that $C_{01} = 0$ as fitting the $\hat{u}$ component doesn't require any intercept term since $\hat{u}$ passes through the origin. Now expanding equations (70,71) yields:

$$\vec{u}'_{pred} = \hat{B} \begin{bmatrix} C_{02} \\ C_{03} \\ \vdots \\ C_{(m-n)+1} \end{bmatrix} + \|\vec{m}'\|_2 \, C_{11} \hat{u}_{des} + \|\vec{m}'\|_2 \, \hat{B} \begin{bmatrix} C_{12} \\ C_{13} \\ \vdots \\ C_{(m-n)+1} \end{bmatrix} \Longleftrightarrow \tag{72}$$

$$\vec{u}'_{pred} = \hat{B} \begin{bmatrix} C_{02} \\ C_{03} \\ \vdots \\ C_{(m-n)+1} \end{bmatrix} + \|\vec{m}'\|_2 \, \hat{\mathcal{B}} \begin{bmatrix} C_{11} \\ C_{12} \\ C_{13} \\ \vdots \\ C_{(m-n)+1} \end{bmatrix} \tag{73}$$

where the first term on the right hand side of Eqs (72,73) is a constant offset vector in P_{iso}. Note that comparing Eqs. (59,60) and (72) shows that:

$$\vec{c}_0 = \hat{B} \begin{bmatrix} C_{02} \\ C_{03} \\ \vdots \\ C_{(m-n)+1} \end{bmatrix} = \hat{B}^T_{sat} \left(\hat{B}_{sat} \hat{B}^T_{sat} \right)^{-1} \vec{s}_2 \tag{74}$$

$$\vec{c}_1 = + \|\vec{m}'\|_2 \, \hat{B} \begin{bmatrix} C_{12} \\ C_{13} \\ \vdots \\ C_{(m-n)+1} \end{bmatrix} = -\hat{B}^T_{sat} \left(\hat{B}_{sat} \hat{B}^T_{sat} \right)^{-1} \left(P_{min} \vec{m}^*_{des} \right)_{sat} \tag{75}$$

4. Iterative Algorithm Saturation Assumption

The iterative algorithm described above, functions well numerically in the vast majority of cases. However, this algorithm (as detailed) which proceeds from corner to corner, makes the assumption that once a control effector is saturated, it remains saturated as the amplitude $\|\vec{m}_{des}\|_2$ increases for a given $\hat{m}_{des}$ direction. For an arbitrary given controls effectiveness matrix (B) of robust rank, this assumption has been observed to hold for the vast majority of selected $\hat{m}_{des}$ cases. However, typically on the order of 15% of cases require one or more saturated effectors to periodically unsaturate as the amplitude of $\|\vec{m}_{des}\|_2$ increases. While not described in this paper, a rigorous method has been developed that correctly determines unsaturation cases and correctly updates the list of saturated controls thereby providing highly accurate results for all arbitrary $\hat{m}_{des}$ from the origin to $\delta(\Phi)$.

5. Prediction Method Yields Moore-Penrose Optimal Control Allocation Solutions

It is now readily seen that the prediction algorithm has constructed MP optimal control allocation solutions that are in accordance with Theorems 1 and 2.

Case 1: $\vec{m}_{des} \in \Phi_1$

From equation (38), we know for $\vec{m}_{des} \in \Phi_1$ that the iterative algorithm yields a solution of the form $\vec{u}_{opt} = a_1 \hat{u}_{des}$. Now by equations (12) and (13) we have:

$$\vec{u}_{opt} = a_1 \hat{u}_{des} = a_1 \frac{P_{min} \vec{m}_{des}}{\|P_{min} \vec{m}_{des}\|_2} \implies \tag{76}$$

$$\vec{u}_{opt} = a_1 \left(\frac{1}{\|\vec{m}_{des}\|_2 \, \|P_{min} \hat{m}_{des}\|_2} \right) P_{min} \vec{m}_{des} \tag{77}$$

and since $\|P_{min} \hat{m}_{des}\|_2$ is fixed for a given $\hat{m}_{des}$, then the variation in gain parameter a_1 merely serves to specify the length of the desired moment vector. Similarly from the Moore-Penrose Theorem 1, we know that for $\vec{m}_{des} \in \Phi_1$, the

optimal solution requires $\vec{u}_{opt} \coloneqq P_{min}\vec{m}_{des}$ which when compared to equation (77) shows the iterative algorithm indeed yields the correct optimal solutions from Theorem 1:

$$\vec{u}_{opt} = P_{min}\vec{m}_{des} \iff a_1\hat{u}_{des}, \text{ with } a_1 = \|\vec{m}_{des}\|_2 \, \|P_{min}\hat{m}_{des}\|_2 \tag{78}$$

Case 2: $\vec{m}_{des} \in \Phi_3$

Examining the iterative algorithm solutions for the constrained MP case, we know for a given $\vec{m}_{des}$ (not necessarily at a corner) and associated set of saturated controls S_2 and $\vec{s}_2$, we have from Eqs. (57) and (57):

$$\vec{u}_{opt} = a_1\hat{u}_{des} + \hat{B}\hat{B}_{sat}^T \left(\hat{B}_{sat}\hat{B}_{sat}^T\right)^{-1} (\vec{s}_2 - \vec{a}_{1sat}) \tag{79}$$

However, we have previously shown the since $a_1\hat{u}_{des} \in P_{Smin} \implies \vec{a}_1 = a_1\hat{u}_{des} = P_{min}\vec{m}_{des}$ and therefore

$$\vec{u}_{opt} = P_{min}\vec{m}_{des} + \hat{B}\hat{B}_{sat}^T \left(\hat{B}_{sat}\hat{B}_{sat}^T\right)^{-1} (\vec{s}_2 - (P_{min}\vec{m}_{des})_{sat}) \tag{80}$$

Recalling that the second order sufficient conditions satisfactorily yielded the minimum null-space solution and then comparing equation 80 to the solutions from Theorem 2, we see that:

$$\vec{u}_{\perp min} = \hat{B}\hat{B}_{sat}^T \left(\hat{B}_{sat}\hat{B}_{sat}^T\right)^{-1} (\vec{s}_2 - (P_{min}\vec{m}_{des})_{sat}) \implies \tag{81}$$

$$\vec{u}_{opt} = P_{min}\vec{m}_{des} + \hat{B}\hat{B}_{sat}^T \left(\hat{B}_{sat}\hat{B}_{sat}^T\right)^{-1} (\vec{s}_2 - (P_{min}\vec{m}_{des})_{sat}) \iff \vec{u}_{des} + \vec{u}_{\perp min} \tag{82}$$

and thus for given $\vec{m}_{des}$ and associated sets S_2 and $\vec{s}_2$ (i.e. subset of Φ_3), the iterative algorithm yields solutions in accordance with Theorem 2.

V. Computational Results

In past research, evaluation of a new controls allocation methodology required comparison to existing methods for computational speed and accuracy for both desired moments and optimal control allocation solutions [2][5]. For a given desired moment $\vec{m}_{des}$, the moment accuracy of a particular method which yielded a controls allocation solution of $\vec{u}_{opt}$ is readily assessed as $\left\|\vec{m}_{des} - B\vec{u}_{opt}\right\|_2$. The only challenge in comparing algorithm produced moments to desired moments occurs when the desired moment is unattainable. In these cases, the Durham Direct Allocation (DA) method has been shown to yield exact results and therefore the best comparison would be against the DA maximum achievable moment $\vec{m}_{da}$ which yields $\left\|\vec{m}_{da} - B\vec{u}_{opt}\right\|_2$. The problem of assessing optimal control allocation solutions is more challenging than moment assessment. The highest quality control solution assessment is achieved when comparing an algorithms solution $\vec{u}_{opt}$ against known exact solutions. The exact solutions are readily available for for $\vec{m}_{des} \in \Phi_1$ (e.g. MP generalized inverse solution) or at the extreme boundary of Φ using the Durham Direct Allocation method. This paper proposed proofs that show the nature of the MP optimal solutions and methods to solve for them for $\vec{m}_{des} \in \Phi_3$. Iterative solvers applied to the basic optimization problem (Eqs. 1,4) can only achieve results to within some convergence tolerance (e.g. $\approx 10^{-7}$). Therefore in this paper, results for the Prediction Method (PM) will be compared against eight other standard MP control allocation algorithms for both boundary and interior moment cases. These eight algorithms consist of matlab m-files and are available as on online supplement[8]. The methods include: Dual Branch-Linear Programming Control Allocation (DB-LPCA), Dual Branch-Linear Programming Control Allocation (infinity norm on Control Error Minimization) (DBinf-LPCA), Dual Path-Linear Programming Control Allocation (DP-LPCA), Dual Path-Linear Programming Control Allocation (scaled from boundary) (DPscaled-LPCA), Mixed Optimization-Linear Programming Control Allocation (MO-LPCA), Vertex Jumping Algorithm (VJA), Cascading Generalized Inverse (CGI) and Direct Allocation (DA). For boundary cases the Direct Allocation solution is used for both the moment and exact minimum (unique) controls allocation solution in accordance with:

$$\frac{\|\vec{m}_{da} - \vec{m}_{meth}\|_2}{\|\vec{m}_{da}\|_2} \times 100 \tag{83}$$

$$\frac{\|\vec{u}_{meth}\|_2 - \|\vec{u}_{da}\|_2}{\|\vec{u}_{da}\|_2} \times 100 \tag{84}$$

For known interior cases, the desired moment $\vec{m}_{des}$ is achievable and therefore the moment comparison is readily performed as:

$$\frac{\|\vec{m}_{des} - \vec{m}_{meth}\|_2}{\|\vec{m}_{des}\|_2} \times 100 \tag{85}$$

Unfortunately, for interior cases, any attempt to demonstrate that the prediction method yields results which are 2-norm smaller than other methods is hampered by the inability of some other algorithms to first achieve moment accuracy of sufficient quality to enable control magnitude assessment. Since it is shown in the sequel that the prediction method achieves desired moments in the interior with very high accuracy, the prediction method is first used to match the moment achieved by other algorithms (regardless of their ability to achieve $\vec{m}_{des}$) and now that the two method's moments match, the associated control vector magnitudes are assessed as:

$$\frac{\|\vec{u}_{meth}\|_2 - \left\|\vec{u}_{pred}\right\|_2}{\left\|\vec{u}_{pred}\right\|_2} \times 100 \tag{86}$$

Solutions to Eq. (86) which are positive, denote cases for which the PM obtains optimal control allocation solutions with a smaller 2-norm that the other algorithm under comparison.

Additionally in the paper, some basic timing comparison is performed. The eight algorithms utilize Matlab interpreted code (m-files) whereas the prediction method utilizes a Matlab autocoded executable. The autocode is very inflated with not only a large amount of Matlab autocode but also a large amount of additional code by the author (such as performing the Direct Allocation check, storing large amounts of performance data etc..) Additionally, the Prediction Method was executed (by choice) to run from the origin to the boundary along $\hat{m}_{des}$ instead of stopping once $\vec{m}_{des}$ was achieved. This timing comparison was useful to the author for looking at computation time variations due to changes in code. While timing comparisons against other methods is included for completeness, the results should be viewed with healthy uncertainty.

Now that the basis for analyzing results is established, numerical test cases were devised. The basic Moore-Penrose problem formulation (Eq. 4) for performance comparison consisted of a robust rank B matrix with 20 control effectors and 3 moments ($B \in \Re^{3\times 20}$) with upper and lower control effector position limits ($\vec{u}_{lwr}$ and $\vec{u}_{upr}$). Desired test cases were created by first randomly choosing 1024 of the 2^{20} possible permutations of control effectors set either their upper or lower position limits and multiplying each control limit permutation by the control effector matrix B providing $\vec{m}_{perm_i}$. The AMS boundary cases were created by utilizing the Direct Allocation method to obtain the unique boundary solution $\vec{m}_{da_i}$ along the generated $\vec{m}_{perm_i}$ test cases. Interior cases were selected by first finding the smallest moment vector $\vec{m}^{min}_{perm_i}$ along $\hat{m}_{perm_i}$ such that only the first control effector was saturated. Thus $\vec{m}_{perm_i}$ is the largest moment vector along $\hat{m}_{perm_i}$ for which P_{min} provides a solution within the ACS. Now 1024 uniformly distributed random seeds $r_i \in [0, 1], i \in \{1, \cdots, 1024\}$ were created and then the interior cases $\vec{m}_{des} \in \Phi_3$ were found from:

$$\vec{m}_{des_i} = \vec{m}^{min}_{perm_i} + r_i \left(\vec{m}_{da_i} - \vec{m}^{min}_{perm_i}\right) \tag{87}$$

This process resulted in 1024 test case pairs of $\vec{m}_{da_i}$ and $\vec{m}_{des_i}$ (both parallel to $\hat{m}_{perm_i}$) such that $\vec{m}_{da_i} \in \delta(\Phi)$ and $\vec{m}_{des_i} \in \Phi_3$.

Results are presented for the boundary cases in Tables 1-2. For the 1024 maximum moment (boundary cases), the CGI algorithm failed (m-file crashed) on 30 cases (due to matrix singularity issues) and these cases were then excluded from boundary results consideration. The statistical performance of the algorithms for the remaining 994 cases is shown in Table 2. The Prediction Method executable includes ancillary Direct Allocation check code for validating the solution is on the correct boundary object [8], and this check flagged 70 cases in which the PM yielded solutions which were found on the incorrect boundary facet. Therefore the PM results are shown with and without the flagged cases. Table 2, shows that for the 93% of cases for which the PM found the correct boundary facet, the method yielded both moment and control solutions with high accuracy when compared to the DA known exact solutions. For the 7% of cases for which the PM failed to find the boundary surface, the PM stopped short or yielded a solution which was precisely along $\hat{m}_{des}$ but with a 2-norm magnitude less than that of the correct boundary solution. While the online algorithm routines did not include Direct Allocation check code for validating the solution is on the correct boundary object, for comparison purposes a post processing check was performed for the CGI algorithm. This check showed that the CGI algorithm failed to find the correct boundary facet on 417 out of 1024 cases (40.7% failure rate).

Results for interior cases are presented in Tables 3-6 and in Fig. 7. To be noted, the PM computation times are identical in Tables 1 (Boundary) and 3 (Interior). This is due to choice to have the PM algorithm run from origin to

boundary regardless of $\|\vec{m}\|_2$. Table 4 shows that the MO-LPCA and CGI algorithms had the most difficulty in achieving the interior moment $\vec{m}_{des}$. Looking at the mean error percentage results in Table 4, shows that the PM algorithm achieved lower control magnitudes over other algorithms except for the aforementioned algorithms MO-LPCA and CGI. However since both the CGI and MO-LPCA methods did not consistently achieve the desired moment, it is therefore meaningless to compare control magnitudes at different moment magnitudes. To resolve this, the PM method was applied to the respective moments actually achieved $\vec{m}_{meth_i}$ for all test cases and all algorithms. The results in Table 5 show that the PM method was able to achieve the respective moments for each test case for all algorithms which enables valid control error percentage assessment. Table 5 shows that the mean control magnitude error was now positive for all methods including MO-LPCA. These results are shown in graph form in Figure 7. Finally, Table 6 counts the number of cases for which an algorithm produced a lower control magnitude than the corresponding PM case results. Tables 3-6 show that with the exception of the CGI algorithm, for equivalent moment magnitudes, the PM algorithm consistently achieved lower control magnitudes by very substantial margins. Closer examination of the CGI algorithm in Tables 4–6, show that the mean control percent error for CGI was approximately centered around zero with half the cases producing larger control magnitudes and half the case producing lower control magnitudes than the PM algorithm. This is not unexpected since the PM and CGI algorithms have a similar algorithm methodology.

VI. Conclusions

The proposed optimal control Prediction Method for control allocation was derived with a strong theoretical background and yields proven minimum control allocation magnitudes when utilizing the correct list of saturated controls S_2. This baseline Moore-Penrose PM method was expanded to include any positive definite (semidefinite) weighting matrix W_{gi} thereby enhancing the PM method to apply to any generalized inverse (see Appendix D).

Substantial numerical comparison of the Prediction Method against eight other control allocation algorithms was performed for a real-word representative problem consisting of a controls effector matrix with 20 effectors and 3 desired moments, $B \in \Re^{3\times 20}$. These numerical results show that the PM algorithm consistently achieved lower control allocation magnitudes over Linear Programming, Direct Allocation and the Vertex Jumping algorithms for interior moment test cases. PM performance was shown to achieve control amplitudes highly consistent with the Cascading Generalized Inverse method for interior test cases. This should be expected as both algorithms have a very common approach: proceed iteratively along $\hat{m}_{des}$ and perform a local optimization using the latest set of saturated controls. The CGI algorithm performs the local optimization using a reduced size generalized inverse whereas the PM method performs the similar local optimization using a subset of the null-space basis vectors.

Two follow on research papers by this author introduce a Moore-Penrose affine generalized inverse of the form:

$$\vec{u}_{opt} = P_{aff}\vec{m}_{des} + \vec{c}_0, \quad \vec{m}_{des} \in \Phi \tag{88}$$

The MP affine generalized inverse is shown to yield identical solutions to the PM optimal control allocation solutions. Moreover, the MP affine generalized inverse yields 2-norm optimal control allocations in a nearby neighborhood of $\vec{m}_{des} \in \phi \subset \Phi_3$. Specifically this inverse provides optimal solutions near $\vec{m}_{des}$ but allowing for permutations in the direction of $\hat{m}_{des}$ and or the magnitude of $\vec{m}_{des}$. Additionally, the analytic method to ensure the PM method utilizes the closest boundary (i.e. correct set S_2) is described in detail. Furthermore, a closer comparison of the Cascading Generalized Inverse and Prediction Method algorithms is made.

Table 1 Computation Time (secs) for Maximum Moment (Φ Boundary), B: 3x20 1024 Cases

Method	Mean	Std Dev	Max	Min
PM	+7.036E-03	+2.009E-03	+1.655E-02	+4.988E-03
DB-LPCA	+2.450E-03	+5.772E-04	+6.012E-03	+1.264E-03
DBinf-LPCA	+2.580E-02	+4.281E-02	+1.460E-01	+1.811E-03
DP-LPCA	+2.387E-03	+5.990E-04	+5.610E-03	+9.675E-04
DPscaled-LPCA	+2.243E-03	+6.142E-04	+7.954E-03	+1.175E-03
MO-LPCA	+9.673E-04	+4.094E-04	+6.118E-03	+4.832E-04
VJA	+8.102E-04	+1.666E-04	+2.107E-03	+5.810E-04
CGI	+3.546E-03	+7.067E-04	+1.424E-02	+3.031E-03
DUR-DA	+1.472E-02	+9.892E-03	+4.503E-02	+5.514E-04

Table 2 Moment and Control Percent Error at Maximum Moment (Φ Boundary), B: 3x20 994 Cases

$$\frac{\left\|\vec{M}_{DA}-\vec{M}_{METH}\right\|_2}{\left\|\vec{M}_{DA}\right\|_2}\times 100 \qquad \frac{\left\|\vec{U}_{METH}\right\|_2-\left\|\vec{U}_{DA}\right\|_2}{\left\|\vec{U}_{DA}\right\|_2}\times 100$$

Method	Mean	Std Dev	Min	Mean	Std Dev	Min
PM	+2.684E-03	+2.336E-02	+7.903E-15	-8.323E-02	+4.828E-01	-5.294E+00
PM (exc 70 DA)	+1.635E-12	+3.970E-12	+7.903E-15	+2.631E-13	+2.073E-11	-9.962E-11
DB-LPCA	+2.651E-14	+1.558E-14	+0.000E+00	+1.420E+01	+8.671E+01	-1.599E+01
DBinf-LPCA	+9.074E-14	+8.765E-13	+0.000E+00	+4.744E+02	+5.269E+03	-1.464E+01
DP-LPCA	+3.799E-14	+1.645E-14	+0.000E+00	-4.619E-13	+4.266E-12	-1.093E-10
DPscaled-LPCA	+2.845E-14	+1.844E-14	+0.000E+00	-2.756E-16	+2.551E-14	-1.195E-13
MO-LPCA	+5.309E+01	+2.588E+01	+2.675E+00	-5.086E+01	+2.121E+01	-9.995E+01
VJA	+4.059E-03	+4.971E-02	+0.000E+00	-5.776E-02	+4.541E-01	-5.928E+00
CGI	+7.517E-02	+1.487E-01	+0.000E+00	-3.155E-01	+1.047E+00	-6.930E+00

Table 3 Computation Time (secs) for Desired Moment (Φ Interior), B: 3x20 1024 Cases

Method	Mean	Std Dev	Max	Min
PM	+7.036E-03	+2.009E-03	+1.655E-02	+4.988E-03
DB-LPCA	+2.903E-03	+7.222E-04	+7.708E-03	+1.363E-03
DBinf-LPCA	+3.648E-02	+4.877E-02	+4.963E-01	+2.776E-03
DP-LPCA	+1.759E-03	+4.260E-04	+4.074E-03	+1.067E-03
DPscaled-LPCA	+2.186E-03	+6.035E-04	+5.774E-03	+1.131E-03
MO-LPCA	+8.395E-04	+3.141E-04	+4.171E-03	+4.654E-04
VJA	+7.263E-04	+1.734E-04	+2.158E-03	+4.974E-04
CGI	+1.549E-03	+6.719E-04	+8.198E-03	+6.454E-04
DUR-DA	+1.432E-02	+9.858E-03	+4.598E-02	+4.307E-04

Table 4 Moment and Control Percent Error at Desired Moment (Φ Interior), B: 3x20 1024 Cases

$$\frac{\left\|\vec{M}_{DES}-\vec{M}_{METH}\right\|_2}{\left\|\vec{M}_{DES}\right\|_2}\times 100 \qquad \frac{\left\|\vec{U}_{METH}\right\|_2-\left\|\vec{U}_{PRED}\right\|_2}{\left\|\vec{U}_{PRED}\right\|_2}\times 100$$

Method	Mean	Std Dev	Min	Mean	Std Dev	Min
PM	+2.055E-13	+7.270E-13	+0.000E+00	+0.000E+00	+0.000E+00	+0.000E+00
DB-LPCA	+7.012E-14	+1.373E-13	+0.000E+00	+1.277E+02	+5.768E+02	-1.280E-01
DBinf-LPCA	+7.927E-14	+1.288E-13	+0.000E+00	+9.761E+01	+3.931E+02	-2.553E+00
DP-LPCA	+1.774E-13	+3.369E-13	+3.218E-15	+4.910E+02	+1.220E+03	-1.280E-01
DPscaled-LPCA	+2.758E-14	+1.735E-14	+0.000E+00	+2.658E+01	+1.048E+01	+1.346E+00
MO-LPCA	+4.807E+01	+3.212E+01	+0.000E+00	-1.281E+01	+4.910E+01	-9.995E+01
VJA	+2.234E-14	+1.612E-14	+0.000E+00	+2.651E+01	+1.049E+01	+1.320E+00
CGI	+3.307E-04	+1.058E-02	+0.000E+00	+2.043E-03	+7.819E-02	-1.154E+00
DUR-DA	+2.191E-14	+1.201E-14	+0.000E+00	+2.658E+01	+1.048E+01	+1.346E+00

Table 5 Moment and Control Percent Error at Respective Method Moments (Φ Interior), B: 3x20 1024 Cases

$$\frac{\left\|\vec{M}_{PRED}-\vec{M}_{Meth}\right\|_2}{\left\|\vec{M}_{Meth}\right\|_2}\times 100 \qquad \frac{\left\|\vec{U}_{METH}\right\|_2-\left\|\vec{U}_{Pred}\right\|_2}{\left\|\vec{U}_{PRED}\right\|_2}\times 100$$

Method	Mean	Std Dev	Min	Mean(%)	Std Dev(%)	Min(%)
DB-LPCA	+2.072E-13	+8.522E-13	+0.000E+00	+1.277E+02	+5.768E+02	-1.280E-01
DBinf-LPCA	+1.965E-13	+7.952E-13	+0.000E+00	+9.761E+01	+3.931E+02	-2.553E+00
DP-LPCA	+2.175E-13	+9.215E-13	+0.000E+00	+4.910E+02	+1.220E+03	-1.280E-01
DPscaled-LPCA	+1.971E-13	+7.484E-13	+0.000E+00	+2.658E+01	+1.048E+01	+1.346E+00
MO-LPCA	+6.006E-14	+2.085E-13	+0.000E+00	+7.076E+01	+3.444E+01	+5.027E+00
VJA	+1.948E-13	+6.463E-13	+4.559E-15	+2.651E+01	+1.049E+01	+1.320E+00
CGI	+1.956E-13	+6.188E-13	+0.000E+00	+3.462E-03	+6.995E-02	-7.537E-03
DUR-DA	+2.199E-13	+9.496E-13	+3.084E-15	+2.658E+01	+1.048E+01	+1.346E+00

Table 6 Number of cases with Control Error % < 0 , B: 3x20 1024 Cases

$$\frac{\left\|\vec{U}_{METH}\right\|_2-\left\|\vec{U}_{Pred}\right\|_2}{\left\|\vec{U}_{PRED}\right\|_2}\times 100 < 0$$

Method	Des Moment	Resp Moment
DB-LPCA	1	1
DBinf-LPCA	3	3
DP-LPCA	2	2
DPscaled-LPCA	0	0
MO-LPCA	613	0
VJA	0	0
CGI	498	484
DUR-DA	0	0

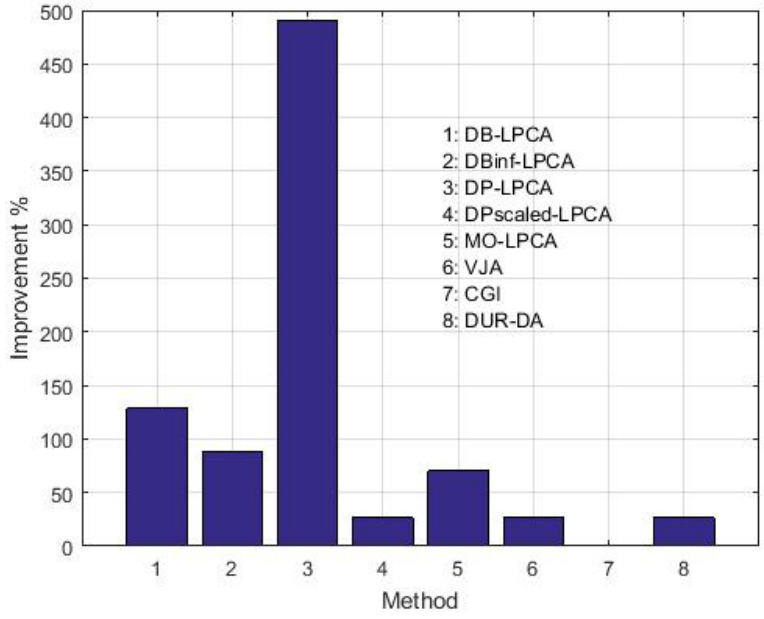

Fig. 7 Percent Improvement of Control Magnitude Using Prediction Method (Φ Interior)

A. Theorems and Proofs

Theorem 1. *Given $\vec{m}_{des} \in \Re^n$ and controls effectiveness matrix $B \in \Re^{n\times m}$, then $\exists! \vec{u}_{opt} = \vec{u}_{des} \coloneqq P_{min}\vec{m}_{des}$ which is the unique minimum 2-norm control such that $B\vec{u}_{opt} = \vec{m}_{des}$.*

Proof. First to show that $B\vec{u}_{opt} = \vec{m}_{des}$ for $\vec{u}_{opt} \coloneqq P_{min}\vec{m}_{des}$. Recalling that for a given control effectiveness matrix B, the Moore-Penrose generalized inverse is $P_{min} \coloneqq B^T\left(BB^T\right)^{-1}$ which shows that: $B\vec{u}_{opt} = BB^T\left(BB^T\right)^{-1}\vec{m}_{des} = \vec{m}_{des}$ as desired. Now to show that $\vec{u}_{opt}$ is the unique minimum 2-norm solution. Assume $\exists \vec{w} \neq \vec{u}_{des}$ such that $B\vec{w} = \vec{m}_{des}$ with $\|\vec{w}\|_2 \leq \|\vec{u}_{des}\|_2$. Then we can find some vector $\vec{v}$ such that $\vec{w} = \vec{u}_{des} + \vec{v}, \vec{v} \neq \vec{0}$. Since the control space is divided into two subspaces: $\mathcal{N}(B)$ and the span of the columns of P_{Smin}, then without loss of generality, we can assume $\vec{v}$ is in either of the subspaces. Let $\vec{v} \in \mathcal{N}(B)$, then since $B\vec{v} = 0 \implies B\vec{w} = B(\vec{u}_{des} + \vec{v}) = \vec{m}_{des}$. However examining $\|\vec{w}\|_2$ we have:

$$\begin{aligned}\|\vec{w}\|_2^2 = \|\vec{u}_{des} + \vec{v}\|_2^2 &\coloneqq \langle \vec{u}_{des} + \vec{v}, \vec{u}_{des} + \vec{v}\rangle \\ &= \|\vec{u}_{des}\|_2^2 + \langle \vec{u}_{des}, \vec{v}\rangle + \langle \vec{v}, \vec{u}_{des}\rangle + \|\vec{v}\|_2^2 \end{aligned} \tag{89}$$

But since $\vec{u}_{des} \in P_{Smin}$ and $\vec{v} \in \mathcal{N}(B)$ we have $\langle \vec{u}_{des}, \vec{v}\rangle = \langle \vec{v}, \vec{u}_{des}\rangle = 0$. Now rearranging Eq. (89):

$$\begin{aligned}&\|\vec{u}_{des}\|_2^2 = \|\vec{w}\|_2^2 - \|\vec{v}\|_2^2 \text{ since } \|\vec{v}\|_2^2 > 0 \implies \\ &\|\vec{u}_{des}\|_2^2 < \|\vec{w}\|_2^2 \implies \|\vec{u}_{des}\|_2 < \|\vec{w}\|_2\end{aligned}$$

So if $\vec{v} \in \mathcal{N}(B)$ then $\vec{w}$ does indeed satisfy $B\vec{w} = \vec{m}_{des}$ but has a larger 2-norm magnitude. Now let $\vec{v} \in$ span of P_{Smin} and since for the Moore-Penrose generalized inverse $BP_{min} = I$ we have:

$$\begin{aligned}&B(\vec{w}) = B(\vec{u}_{des} + \vec{v}) = BP_{min}\vec{m}_{des} + B\vec{v} \\ &\forall \vec{v} \in \text{ span of } P_{Smin} \implies B\vec{v} \neq \vec{0} \implies B\vec{w} = \vec{m}_{des} + B\vec{v} \neq \vec{m}_{des}\end{aligned}$$

Thus the assumption $\exists \vec{w} \neq \vec{u}_{des}$ that satisfies $B\vec{w} = \vec{m}_{des}$ with $\|\vec{w}\|_2 \leq \|\vec{u}_{des}\|_2$ is contradicted in all cases. Therefore $\vec{u}_{opt} = \vec{u}_{des}$ is the unique minimum 2-norm control such that $B\vec{u}_{opt} = \vec{m}_{des}$ as claimed. □

Note the above proposition is merely a reformulation of the well known fact that the Moore-Penrose generalized inverse provides the unique-minimum control vector for the unconstrained case and is included using this paper's terminology for completeness. Now to examine the control position rectilinearly constrained case.

Theorem 2. *Given $\vec{m}_{des} \in \Phi$, $\vec{u}_{lwr} \in \Re^m$ and $\vec{u}_{upr} \in \Re^m$ such that $\vec{u}_{lwr} <= \vec{u}_{upr}$ element wise, then $\exists! \vec{u}_{opt} = \vec{u}_{des} + \vec{u}_{\perp min}$, $\vec{u}_{\perp min} \in P_{iso}$ which is the unique minimum 2-norm control such that $B\vec{u}_{opt} = \vec{m}_{des}$ and $\vec{u}_{lwr} <= \vec{u}_{opt} <= \vec{u}_{upr}$ element wise.*

Proof. Given $\vec{m}_{des} \in \Phi$ then by Eq. (9) we have the existence of at least a solution $\vec{u}^*$ such that $B\vec{u}^* = \vec{m}_{des}$ where $\vec{u}^* \in \Omega$ or equivalently $\vec{u}_{lwr} \leq \vec{u}^* \leq \vec{u}_{upr}$ element wise. It remains to determine the $\vec{u}^*$ which is unique and 2-norm minimal for each $\vec{m}_{des} \in \Phi$. Now by equation (26) either $\vec{u}^* \in \Omega_2$ or $\vec{u}^* \in \Omega_4$.

Case 1: $\vec{u}^* \in \Omega_2$
Recalling the definitions of the subsets Ω_1 and Ω_2 in equations 18,19, then $\forall \vec{u}^* \in \Omega_2, !\exists \vec{u} \in \Omega_1$ where $\vec{u} = \mathcal{P}_{S_{min}}\vec{u}^*$. In fact, by definition of Ω_2, there may be uncountably many $\vec{u}' \in \Omega_2$ such that $\vec{u} = \mathcal{P}_{S_{min}}\vec{u}^* = \mathcal{P}_{S_{min}}\vec{u}'$. However the vectors $\vec{u}^*, \vec{u}' \in \Omega_2$ are just $\vec{u}$ plus a null space vector (e.g. $\vec{u}^* = \vec{u} + \vec{v}$). Since $\vec{u} \in P_{Smin}$ and $\vec{v} \in P_{Iso}$, then $\vec{v} \perp \vec{u}$ and thus

$$\|\vec{u}^*\|_2^2 = \|\vec{u} + \vec{v}\|_2^2 \implies \|\vec{u}\|_2 < \|\vec{u}^*\|_2 \tag{90}$$

Now since both $\vec{u}^*$ and $\vec{u}$ generate the same moment $B\vec{u}^* = B\vec{u} = \vec{m}_{des}$, then $\vec{u}$ is the unique 2-norm minimal vector that satisfies $B\vec{u} = \vec{m}_{des}$. Also by definition of Ω_1 we have $\vec{u} \in \Omega$ and thus the $\vec{u}_{lwr} <= \vec{u} <= \vec{u}_{upr}$ element wise. Now since $\vec{u} \in \Omega_1 \implies \vec{u} \in P_{S_{min}}$ then by Eq. 28 we have $\vec{u} = P_{min}B\vec{u} = P_{min}\vec{m}_{des}$. Therefore $\vec{u} = \vec{u}_{opt} = P_{min}\vec{m}_{des}$ yields a unique 2-norm minimal vector such that $B\vec{u}_{opt} = \vec{m}_{des}$ and $\vec{u}_{lwr} <= \vec{u}_{opt} <= \vec{u}_{upr}$ element wise.

Case 2: $\vec{u}^* \in \Omega_4$ We know that for given $\vec{m}_{des}$ and $\vec{u}^* \in \Omega_4$ then we must have $B\vec{u}^* = \vec{m}$. Since we know that $\forall \vec{u}, B \circ \mathcal{P}_{P_{min}}\vec{u} = B\vec{u}$ and $\mathcal{P}_{P_{min}}\vec{u} \in P_{Smin}$, then $\forall \vec{u}^* \in \Omega_4, \exists \vec{u} \in P_{Smin}, B\vec{u}^* = B\vec{u} = \vec{m}$. Furthermore, we know that

$\vec{u} \in \Omega^C$ by Eq. (21), so then $\vec{u} \notin \Omega$. Now geometrically, we seek to show the existence and uniqueness of the $\vec{v} \in P_{iso}$ with the smallest 2-norm such that $\vec{u} + \vec{v} \in \delta(\Omega_4)$.

In order to accomplish this, we define Ω using the standard Euclidean basis vectors as:

$$\Omega \coloneqq \{\vec{p} \in \Re^m | \vec{p} = \sum_{i=1}^{m} a_i \hat{e}_i, a_i \in \left[\vec{u}_{lwr_i}, \vec{u}_{upr_i}\right]\} \tag{91}$$

then given a point $\vec{w} \in \Re^m$, then we can define the minimum distance to Ω as:

$$d(\vec{w}, \Omega) = \inf\{\|\vec{w} - \vec{y}\|_2 \, | \vec{y} \in \Omega\} \tag{92}$$

We know from Euclidean geometry [9] that this minimal distance exists from the point $\vec{w}$ to a closed and bounded set such as Ω. Now the previous selection of basis vectors $\hat{e}_i$ used in Eq. (91) was arbitrary but convenient based on the limits $\vec{u}_{lwr}$ and $\vec{u}_{upr}$. We can redefine a second set of basis vectors that similarly span $\Re^m$ using the columns of P_{min} and $\hat{B}$. Using the Gram-Schmidt process on the column vectors of P_{min}, we can create an orthonormal basis $\hat{P}$ (basis vectors $\hat{p}_1, \ldots, \hat{p}_n$) which together with $\hat{B}$ forms a complete orthonormal basis for $\Re^m$. Now we can rewrite Ω using this new basis (with the control limits rewritten as linear combinations of $\vec{u}_{lwr}$ and $\vec{u}_{upr}$) as:

$$\Omega \coloneqq \{\vec{p} \in \Re^m | \vec{p} = \sum_{1}^{n} f_i \hat{p}_i + \sum_{1}^{m-n} g_i \hat{b}_i, f_i = \mathcal{F}_i\left(\vec{u}_{lwr_1}, \ldots, \vec{u}_{lwr_m}, \vec{u}_{upr_1}, \ldots, \vec{u}_{upr_m}\right), \tag{93}$$

$$g_i = \mathcal{G}_i\left(\vec{u}_{lwr_1}, \ldots, \vec{u}_{lwr_m}, \vec{u}_{upr_1}, \ldots, \vec{u}_{upr_m}\right)\} \tag{94}$$

Now the change of basis did not alter the set Ω nor did it alter the geometric property that it is closed and bounded and therefore the mimimum distance defined in Eq. (92) still exists. Now focusing on the subset Ω_4, we know that it is bounded but not closed since it doesn't contain the limit points where Ω_4 adjoins to Ω_2. In particular, this boundary between Ω_4 and Ω_2 is defined in the direction of $P_{S_{min}}$ (i.e. it can not be approached using $\hat{B}$ but only by using $\hat{P}$), therefore we can form a closed and bounded subset of interest in Ω_4 for a given point $\vec{u} \in P_{S_{min}}$ if we fix the point $\vec{u} \coloneqq P_{min}\vec{m} = \sum_1^n f_i \hat{p}_i$ and then define:

$$\Omega_{\vec{u}} \coloneqq \{\vec{p} \in \Re^m | \vec{p} = \vec{u} + \sum_{1}^{m-n} g_i \hat{b}_i, \vec{u} \coloneqq P_{min}\vec{m}, g_i = \mathcal{G}_i\left(\vec{u}_{lwr_1}, \ldots, \vec{u}_{lwr_m}, \vec{u}_{upr_1}, \ldots, \vec{u}_{upr_m}\right)\} \subset \Omega_4 \tag{95}$$

and similarly:

$$d(\vec{u}, \Omega_{\vec{u}}) = \inf\{\|\vec{u} - \vec{y}\|_2 \, | \vec{y} \in \Omega_{\vec{u}}\} \tag{96}$$

Therefore Eqs. (95,96), show that there exists a 2-norm minimal $\vec{v} \in P_{iso}$ with length $\|\vec{v}\|_2 = d(\vec{u}, \Omega_{\vec{u}})$ such that $\vec{u} + \vec{v} \in \Omega_{\vec{u}}$. At this time, we don't know if the vector $\vec{v}$ is unique. For this, we appeal to the fact that the set $\Omega_{\vec{u}}$ is closed and convex (since it has all linear sides), and therefore the solution to Eq. (96) is unique [9]. Now we know a unique solution exists but we must construct it from the endpoint of the vector $\vec{u} \in P_{Smin}$ to the closest boundary. The closest boundary of Ω_4 is a closed subset of a rectilinear hyperspace (of some dimension and at some orientation) which can be completely reached using $\hat{B}$. Now to find the distance between a point and a rectilinear hyperspace we use the projection operator which we know produces a unique projection vector $\vec{u}_p$ and therefore we have produced a unique vector $\vec{v}$ from $\vec{u}$ to the projection vector $\vec{u}_p$ as: $\vec{v} \coloneqq \vec{u} - \mathcal{P}_{\delta(\Omega_4)}\vec{u}$.

It should be noted that the set $\Omega_{\vec{u}}$ is the only subset of Ω_4 that contains all vectors which $\forall \vec{w} \in \Omega_{\vec{u}}, B\vec{w} = B\vec{u}^* = \vec{m}$ since the moment is strictly determined by $B\vec{u}$. Thus using $\vec{u} = P_{min}\vec{m}$ and $\vec{v} \in P_{iso}$ generated by $\Omega_{\vec{u}}$ together with $\vec{u} \perp \vec{v}$ implies:

$$\|\vec{u} + \vec{v}\|_2 \coloneqq \|\vec{u}\|_2 + \|\vec{v}\|_2 \tag{97}$$

Thus for fixed $\vec{u}$ (necessary to achieve $\vec{m}$) with the minimal length $\vec{v}$ then Eq. (97) is minimized which implies by definition of Ω_3 in Eq. (20) that $\vec{u} + \vec{v} \in \Omega_3$.

So finally, for all $\vec{m} \in \Phi_3$, we have a $\vec{u}^* \in \Omega_4$ which generates a corresponding unique $\vec{u} \coloneqq P_{min}\vec{m} \in P_{S_{min}}$ which is used to define the subset $\Omega_{\vec{u}} \subset \Omega_4$ which yields a minimal 2-norm vector $\vec{v}$ with the following simultaneous properties:

$$B(\vec{u} + \vec{v}) = \vec{m} \tag{98}$$

$$\vec{v} \in P_{iso} \tag{99}$$

$$\|\vec{u} + \vec{v}\|_2 < \|\vec{w}\|_2, \forall \vec{w} \in \Omega_{\vec{u}}, \vec{w} \neq \vec{u} + \vec{v} \tag{100}$$

$$(\vec{u} + \vec{v}) \in \Omega_{\vec{u}} \subset \Omega_4 \implies \vec{u}_{lwr} \leq (\vec{u} + \vec{v}) \leq \vec{u}_{upr} \text{ (element wise)} \tag{101}$$

Now the above is true for all $\vec{m} \in \Phi_3$, and thus case 2 is also proven as claimed. Moreover, we know that the set Ω_3 contains only MP optimal control allocation solutions and that both the subsets Ω_3, Ω_4 linearly transform by B onto Φ_3. □

B. ACS and AMS Subset Relationships

Recalling the ACS and AMS subsets and their important relationships, we have:

$$\Omega_1 \coloneqq \{\vec{u} \in \Omega \cap P_{Smin}\} \tag{102}$$
$$\Omega_2 \coloneqq \{\vec{u} \in \Omega | \mathcal{P}_{P_{min}} \vec{u} \in \Omega \cap P_{Smin}\} \tag{103}$$
$$\Omega_3 \coloneqq \{\vec{u} \in \Omega_4 | \forall \vec{u}' \in \Omega_4 \text{ where } \mathcal{P}_{P_{min}} \vec{u} = \mathcal{P}_{P_{min}} \vec{u}', \|\vec{u}\|_2 < \|\vec{u}'\|_2\} \tag{104}$$
$$\Omega_4 \coloneqq \{\vec{u} \in \Omega | \mathcal{P}_{P_{min}} \vec{u} \in \Omega^C \cap P_{Smin}\} \tag{105}$$

and similarly the Attainable Moment Set Φ is divided into two subsets as follows:

$$\Phi_1 \coloneqq \{\vec{m} \in \Phi | \vec{u} \in \Omega_1, B\vec{u} = \vec{m}\} \tag{106}$$
$$\Phi_3 \coloneqq \{\vec{m} \in \Phi | \vec{u} \in \Omega_3, B\vec{u} = \vec{m}\} \tag{107}$$

Some important relationships among the above subsets are:

$$\Omega_1 \subset \Omega_2 \tag{108}$$
$$\Omega_3 \subset \Omega_4 \tag{109}$$
$$\Omega_2 \cup \Omega_4 = \Omega \text{ and } \Omega_2 \cap \Omega_4 = \emptyset \tag{110}$$
$$\forall \vec{m} \in \Phi \implies BP_{min}\vec{m} = \vec{m} \in \Re^n \tag{111}$$
$$\forall \vec{u} \in \Omega_1 \quad P_{min}B\vec{u} = \vec{u} \in \Re^m \tag{112}$$
$$\Phi_1 \cup \Phi_3 = \Phi \text{ and } \Phi_1 \cap \Phi_3 = \emptyset \tag{113}$$

First to show Eq. (108) that $\Omega_1 \subset \Omega_2$:

Proof. For $\vec{u} \in \Omega_1 \implies \vec{u} \in \Omega \cap P_{Smin} \implies \vec{u} \in P_{Smin}$. Since $\vec{u}$ is in the MP surface then the orthogonal projection of $\vec{u}$ onto the MP surface leaves $\vec{u}$ unchanged (ie. $\vec{u} \in P_{Smin} \implies \vec{u} = \mathcal{P}_{P_{min}} \vec{u}$). Since $\vec{u}$ is unchanged under the projection operation then $\vec{u} \in \Omega \cap P_{Smin} \implies \mathcal{P}_{P_{min}} \vec{u} \in \Omega \cap P_{Smin}$. So $\Omega_1 \subset \Omega_2$ as claimed. □

Equation 109 follows directly since $\forall \vec{u} \in \Omega_3 \subset \Omega_4$ by definition of Ω_3. Demonstration of Eq. (110) is:

Proof. First to prove: $\Omega_2 \cup \Omega_4 = \Omega$. Combining the sets Ω_2 and Ω_4 yields:

$$\begin{aligned}
\Omega_2 \cup \Omega_4 &= \{\vec{u} \in \Omega | \mathcal{P}_{P_{min}} \vec{u} \in \Omega \cap P_{Smin}\} \cup \{\vec{u} \in \Omega | \mathcal{P}_{P_{min}} \vec{u} \in \Omega^C \cap P_{Smin}\} \\
&= \{\vec{u} \in \Omega | \mathcal{P}_{P_{min}} \vec{u} \in \{\Omega \cap P_{Smin} \cup \Omega^C \cap P_{Smin}\}\} \\
&= \{\vec{u} \in \Omega | \mathcal{P}_{P_{min}} \vec{u} \in \{\Omega \cup \Omega^C\} \cap P_{Smin}\} \\
&= \{\vec{u} \in \Omega | \mathcal{P}_{P_{min}} \vec{u} \in P_{Smin}\} \text{ which combined with } P_{Smin} \coloneqq \{\mathcal{P}_{P_{min}} \vec{u} | \vec{u} \in \Omega\} \implies \\
\Omega_2 \cup \Omega_4 &= \Omega
\end{aligned}$$

Next $\Omega_2 \cap \Omega_4 = \emptyset$ follows directly since $\forall \vec{u} \in \Omega$ the vector $\mathcal{P}_{P_{min}} \vec{u}$ cannot be in both Ω^C and Ω. Note that $\emptyset \in \Omega$ only. □

Equation (111) follows since for the MP generalized inverse we have $I = BP_{min} \coloneqq B\left(B^T\left(BB^T\right)^{-1}\right)$ and therefore $\forall \vec{m} \in \Phi_1, \quad BP_{min}\vec{m} = \vec{m}$. Note Eq. (111) was shown only for the MP generalized inverse, but it is straightforward to see the same holds for the generalized inverse cases (see Eqs. 2 and 3). Demonstration of Eq. (112) is as follows:

Proof. Recalling that orthogonally projecting any vector from a subspace back onto the same subspace leaves the vector unchanged, so consequently a vector in a subset of the subspace is also unchanged and thus:

$$\vec{u} \in P_{Smin} \implies \vec{u} = \mathcal{P}_{P_{min}}\vec{u} \text{ and since } \mathcal{P}_{P_{min}} \coloneqq B^T\left(BB^T\right)^{-1}B \implies$$
$$\vec{u} = B^T\left(BB^T\right)^{-1}B\vec{u} \text{ however } P_{min} \coloneqq B^T\left(BB^T\right)^{-1} \implies P_{min}B\vec{u} = \vec{u}$$
$$\text{since } \Omega_1 \subset P_{Smin} \implies \forall \vec{u} \in \Omega_1 \implies P_{min}B\vec{u} = \vec{u}$$

So $\forall \vec{u} \in \Omega_1$ we have $P_{min}B\vec{u} = \vec{u}$ as claimed. □

Based on the B mappings between subsets shown in Theorem 2, we can now show Eq. (113). First to show $\Phi_1 \cup \Phi_3 = \Phi$. Recalling that by Eq. (9) together with Eq. (109) then we have $\forall \vec{m} \in \Phi$ either $\vec{m} \in \Omega_2$ or $\vec{m} \in \Omega_4$, but we have shown that Ω_2 is linearly transformed by B onto Φ_1 and similarly Ω_4 is linearly transformed by B onto Φ_3 which implies $\Phi_1 \cup \Phi_3 = \Phi$.

Now to show that $\Phi_1 \cap \Phi_3 = \emptyset$.

Proof. (By Contradiction): Assume $\Phi_1 \cap \Phi_3 \neq \emptyset$, then $\exists \vec{m} \in \Phi_1, \Phi_3$. Now by definition (102), $\exists \vec{u}_1 \in \Omega_1$ such that $B\vec{u}_1 = \vec{m}$ and similarly by definition (107), $\exists \vec{u}_3 \in \Omega_3$ such that $B\vec{u}_3 = \vec{m}$. However, we know that $\forall \vec{u}, B \circ \mathcal{P}_{P_{min}}\vec{u} = B\vec{u}$ and in particular that the vector $\mathcal{P}_{P_{min}}\vec{u}$ contains no portion in $\mathcal{N}(B)$, then since $\vec{m} = B \circ \mathcal{P}_{P_{min}}\vec{u}_1 = B \circ \mathcal{P}_{P_{min}}\vec{u}_3 \implies \mathcal{P}_{P_{min}}\vec{u}_1 = \mathcal{P}_{P_{min}}\vec{u}_3$, or equivalently that the non-nullspace components of $\vec{u}_1$ and $\vec{u}_3$ are identical. However, by definition (102), we must have that $\vec{u}_1 \in \Omega \cap P_{Smin} \implies \vec{u}_1 \in P_{Smin}$. Since $\vec{u}_1 \in P_{Smin}$ then this implies $\vec{u}_1$ is unchanged by the projection operator $\mathcal{P}_{P_{min}}$ and thus $\mathcal{P}_{P_{min}}\vec{u}_1 \in \Omega \cap P_{Smin}$. Similarly by definition (104), we must have that $\vec{u}_3 \in \Omega_4$ which by definition (105), implies that $\mathcal{P}_{P_{min}}\vec{u}_3 \in \Omega^C \cap P_{Smin}$. However, we now have a contradiction since we cannot have $\mathcal{P}_{P_{min}}\vec{u}_1 = \mathcal{P}_{P_{min}}\vec{u}_3$ and $\mathcal{P}_{P_{min}}\vec{u}_1 \in \Omega$ together with $\mathcal{P}_{P_{min}}\vec{u}_3 \in \Omega^C$. Thus $\Phi_1 \cap \Phi_3 = \emptyset$ as claimed. □

C. Moore-Penrose Null-Space Optimization

For the Moore-Penrose generalized inverse problem, the following shows the derivation the minimal null-space vector $\vec{u}_\perp$ to return $\vec{u} = \vec{u}_\parallel + \vec{u}_\perp \in \Omega$.

$$J\left(\vec{b}, \vec{\lambda}\right) \coloneqq \frac{1}{2}\vec{b}^T\vec{b} + \vec{\lambda}^T\left(\vec{a}_{0sat} - \vec{a}_{1sat} - \hat{B}_{sat}\vec{b}\right) \tag{114}$$

where the subscript "sat" refers to only utilizing the row components of the respective vector/matrix that correspond to the current list of saturated controls (S_2). For example, if the saturated controls are $S_2 = \{1, 3, 7\}$ then for the vector $\vec{a}_1 \coloneqq \begin{bmatrix} a_1 & a_2 & \dots & a_m \end{bmatrix}^T$ we have $\vec{a}_{1sat} = \begin{bmatrix} a_1 & a_3 & a_7 \end{bmatrix}^T$.

Now the first order necessary conditions for optimality of Eq. (114) are $\frac{\partial J}{\partial \vec{b}} = \vec{0}$ and $\frac{\partial J}{\partial \vec{\lambda}} = \vec{0}$. Solving for $\frac{\partial J}{\partial \vec{b}}$ yields:

$$\frac{\partial J}{\partial \vec{b}} = \vec{b}^T - \lambda^T\hat{B}_{sat} = \vec{0} \tag{115}$$

and similarly solving for $\frac{\partial J}{\partial \vec{\lambda}}$ yields:

$$\frac{\partial J}{\partial \vec{\lambda}} = \left(\vec{a}_{0sat} - \vec{a}_{1sat} - \hat{B}_{sat}\vec{b}\right)^T = \vec{0} \tag{116}$$

Now rearranging Eq. (115) yields:

$$\vec{b}^T = \vec{\lambda}^T\hat{B}_{sat} \tag{117}$$

and similarly distributing the transpose in Eq. (116) yields:

$$\vec{a}_{0sat}^T - \vec{a}_{1sat}^T - \vec{b}^T\hat{B}_{sat}^T = \vec{0} \tag{118}$$

Now combining Eqs. (117) with (118) and rearranging yields:

$$\lambda^T\hat{B}_{sat}\hat{B}_{sat}^T = \vec{a}_{0sat}^T - \vec{a}_{1sat}^T \tag{119}$$

Now defining k as the number of saturated controls, then $\hat{B}_{sat} \in \Re^{k\times(m-n)}$. Recalling from linear algebra [10] that rank $\left(AA^T\right) =$ rank (A), so then $\left(\hat{B}_{sat}\hat{B}_{sat}^T\right)^{-1}$ exists if $k \leq m-n$ and therefore

$$\vec{\lambda}^T = \left(\vec{a}_{0sat}^T - \vec{a}_{1sat}^T\right)\left(\hat{B}_{sat}\hat{B}_{sat}^T\right)^{-1} \tag{120}$$

Now substituting Eq. (120) into Eq. (117)yields:

$$\vec{b}_{min} = \hat{B}_{sat}^T\left(\hat{B}_{sat}\hat{B}_{sat}^T\right)^{-1}\left(\vec{a}_{0sat} - \vec{a}_{1sat}\right) \tag{121}$$

Thus for a given scalar a_0 and current list of saturated controls, Eq. (121) shows the analytic solution for the null space basis vector gains ($\vec{b}_{min}$) necessary to return $\vec{a}_1$ to $\delta(\Omega)$. Now to look at the second order sufficient criterion to determine if we indeed have a minimal solution. The second order sufficient condition is $\frac{\partial^2 J}{\partial \vec{b}^2} > 0$. Using Eq. (115) then we have $\frac{\partial^2 J}{\partial \vec{b}^2} = I > 0$. Thus the solution from Eq. (121) does indeed yield results that provide the minimum $\|\vec{u}_\perp\|_2$.

D. Generalized Inverse Null-Space Optimization

In this section, the local null space optimization problem with equality constraints that was previously analyzed for Moore-Penrose generalized inverse case is revised to accommodate any (arbitrary) generalized inverse. Given $W_{gi} \in \Re^{m\times m}$ where $W_{gi} > 0$ then defining:

$$P_{gi} \coloneqq W_{gi}^{-1}B^T\left(BW_{gi}^{-1}B^T\right)^{-1} \tag{122}$$

Then the following cost function is examined:

$$J\left(\vec{b},\vec{\lambda}\right) = \frac{1}{2}\vec{u}^T W_{gi}\vec{u} + \vec{\lambda}^T\left(\vec{s}_2 - \vec{a}_{1_{sat}}^{gi} - \hat{B}_{sat}\vec{b}\right) \tag{123}$$

Note the addition of the positive definite weighting matrix W_{gi} and the change in vector $\vec{a}_{1_{sat}}^{gi}$. Specifically, $\vec{a}_{1_{sat}}^{gi}$ is defined as:

$$\vec{a}_{1_{sat}}^{gi} \equiv a_1^{gi}\hat{u}_{sat}^{gi} \text{ where} \tag{124}$$

$$\hat{u}^{gi} \coloneqq \frac{P_{gi}\vec{m}_{des}}{\left\|P_{gi}\vec{m}_{des}\right\|_2} \tag{125}$$

Previously, $\vec{a}_1$ was utilized where:

$$\vec{a}_{1_{sat}} \equiv a_1\hat{u}_{sat} \text{ where} \tag{126}$$

$$\hat{u} \coloneqq \frac{P_{min}\vec{m}_{des}}{\|P_{min}\vec{m}_{des}\|_2} \tag{127}$$

Since the vector we seek is in P_{iso}, then substituting $\vec{u} = \hat{B}\vec{b}$ into Eq. (123) yields:

$$J\left(\vec{b},\vec{\lambda}\right) = \frac{1}{2}\vec{b}^T\left(\hat{B}^T W_{gi}\hat{B}\right)\vec{b} + \vec{\lambda}^T\left(\vec{s}_2 - \vec{a}_{1_{sat}}^{gi} - \hat{B}_{sat}\vec{b}\right) \tag{128}$$

Now proceeding with the Necessary First Order Conditions for optimality yield:

$$\frac{\partial J}{\partial \vec{b}} = \vec{b}^T\hat{B}^T W_{gi}\hat{B} + \lambda^T\hat{B}_{sat} = 0 \tag{129}$$

$$\frac{\partial J}{\partial \vec{\lambda}} = \left(\vec{s}_2^T - \vec{a}_{1_{sat}}^{gi^T} - \vec{b}_{sat}^T\hat{B}_{sat}^T\right) = 0 \tag{130}$$

Now to show that $\left(\hat{B}^T W_{gi}\hat{B}\right)^{-1}$ exists $\forall W_{gi} > 0$. Since $W_{gi} > 0$ then the singular value decomposition takes the form $W_{gi} = UDU^T$ with U a column matrix of orthonormal eigenvectors and D a diagonal matrix whose diagonal

elements are the strictly positive real eigenvalues of W_{gi}. Therefore W_{gi} can be decomposed into $W_{gi} = \Lambda^{1/2}\Lambda^{1/2}$ where:

$$\Lambda^{1/2} = UD^{1/2}U^T, \text{ where } D^{1/2} = \begin{bmatrix} \sqrt{D_{1,1}} & 0 & 0 & 0 \\ 0 & \sqrt{D_{2,2}} & 0 & 0 \\ 0 & 0 & \ddots & 0 \\ 0 & 0 & 0 & \sqrt{D_{m,m}} \end{bmatrix} \tag{131}$$

Now using $\Lambda^{1/2} = \Lambda^{1/2^T}$ together with $W_{gi} = \Lambda^{1/2}\Lambda^{1/2}$, then $\left(\hat{B}^T W_{gi}\hat{B}\right)$ is:

$$\left(\hat{B}^T W_{gi}\hat{B}\right) = \left(\left(\Lambda^{1/2}\hat{B}\right)^T \left(\Lambda^{1/2}\hat{B}\right)\right) \tag{132}$$

From linear algebra we know that $dim\mathcal{N}(A) = dim\mathcal{N}\left(A^T A\right)$ [10]. So then with $A = \Lambda^{1/2}\hat{B}$ we have $dim\mathcal{N}\left(\hat{B}^T W_{gi}\hat{B}\right) = dim\mathcal{N}\left(\Lambda^{1/2}\hat{B}\right)$. Since $\mathcal{N}\left(\Lambda^{1/2}\right) = \emptyset$ and $\mathcal{N}\left(\hat{B}\right) = \emptyset$ then $\mathcal{N}\left(\Lambda^{1/2}\hat{B}\right) = dim\mathcal{N}\left(\hat{B}^T W_{gi}\hat{B}\right) = \emptyset \implies \exists!\left(\hat{B}^T W_{gi}\hat{B}\right)^{-1} \forall W_{gi} > 0$.

Next Eq. (129) implies:

$$\vec{b}^T = -\vec{\lambda}^T \hat{B}_{sat}\left(\hat{B}^T W_{gi}\hat{B}\right)^{-1} \tag{133}$$

Now substituting Eq. (133) into Eq. (130) yields:

$$0 = \left(\vec{s}_2^T - \vec{a}_{1_{sat}}^{gi^T}\right) + \vec{\lambda}^T \hat{B}_{sat}\left(\hat{B}^T W_{gi}\hat{B}\right)^{-1}\hat{B}^T \implies \tag{134}$$

$$\vec{\lambda}^T = -\left(\vec{s}_2^T - \vec{a}_{1_{sat}}^{gi^T}\right)\left(\hat{B}_{sat}\left(\hat{B}^T W_{gi}\hat{B}\right)^{-1}\hat{B}_{sat}^T\right)^{-1} \tag{135}$$

Where as before, the inverse $\left(\hat{B}_{sat}\left(\hat{B}^T W_{gi}\hat{B}\right)^{-1}\hat{B}_{sat}^T\right)^{-1}$ exists for $\hat{B}_{sat} \in \Re^{k\times(m-n)}$ if $k \leq (m-n)$ with k defined as the number of saturated controls. Now substituting in Eq. (135) into Eq. (133) and taking the transpose of the result yields:

$$\vec{b}_{gi} = \left(\hat{B}^T W_{gi}\hat{B}\right)^{-1}\hat{B}_{sat}^T\left(\hat{B}_{sat}\left(\hat{B}^T W_{gi}\hat{B}\right)^{-1}\hat{B}_{sat}^T\right)^{-1}\left[\vec{s}_2 - \vec{a}_{1_{sat}}^{gi}\right] \tag{136}$$

So finally $\vec{u}_{opt}$ is:

$$\vec{u}_{opt} = \begin{bmatrix}\hat{u}_{gi} & \hat{B}\end{bmatrix}\begin{bmatrix} a_1^{gi} \\ \vec{b}_{gi}\end{bmatrix} \tag{137}$$

Note that for the for the choice of $W_{gi} = I$, with the fact that $\hat{B}^T\hat{B} = I$ then $\hat{B}^T W_{gi}\hat{B} = \hat{B}^T\hat{B} = I$. Therefore for the special case of $W_{gi} = I$, we recover the $P_{gi} = P_{min}$ and the local optimal basis gains $\vec{b}_{gi} = \vec{b}_{min}$.

Now the sufficient condition for a local minimum requires that: $\frac{\partial^2 J}{\partial \vec{b}^2} > 0$ [11]. Thus taking the partial derivative of equation (129) with respect to $\vec{b}$ yields:

$$\frac{\partial^2 J}{\partial \vec{b}^2} = \frac{\partial}{\partial \vec{b}}\left(\vec{b}^T\hat{B}^T W_{gi}\hat{B} + \lambda^T\hat{B}_{sat}\right) = \hat{B}^T W_{gi}\hat{B} > 0 \tag{138}$$

Since $W_{gi} > 0$ and $\mathcal{N}\left(\hat{B}\right) = 0$ then $\hat{B}\vec{y} = \vec{0} \iff \vec{y} = \vec{0}$. Thus $\vec{y}^T\hat{B}^T W_{gi}\hat{B}\vec{y} > 0$ and the solution found is indeed a local minimum.

Acknowledgments

The author would like to give many thanks to John Foster at NASA Langley, for peaking my curiosity on the subject of Control Allocation and for pointing me on the initial vector to Wayne Durham's seminal paper [1]. Also, a special thank you goes to Bart Bacon at NASA Langley for his very thorough paper review.

References

[1] Durham, W. C., "Constrained Control Allocation," *Journal of Guidance, Control, and Dynamics*, Vol. 16, No. 4, 1994, pp. 717, 725. doi:10.2514/3.21201.

[2] Jin, J., "Modified Pseudoinverse Redistribution Methods for Redundant Controls Allocation," *Journal of Guidance, Control, and Dynamics*, Vol. 28, No. 5, 2005, pp. 1076–1079. doi:10.2514/1.14992.

[3] Enns, D., "Control Allocation Approaches," *AIAA Guidance, Navigation, and Control Conference and Exhibit*, AIAA, Boston, MA, 1998, pp. 98,108.

[4] Bordignon, K. A., *Constrained Control Allocation for Systems with Redundant Control Effectors*, Ph.D. Dissertation, Virginia Polytechnic Institute and State University, Blacksburg, VA, 1996.

[5] Bodson, M., "Evaluation of Optimization Methods for Control Allocation," *AIAA Guidance, Navigation, and Control Conference and Exhibit*, AIAA Paper 2001-4223, 2001. doi:10.2514/6.2001-4223.

[6] Bordignon, K., and Bessolo, J., "Control Allocation For The X-35B," *2002 Biennial International Powered Lift Conference and Exhibit*, AIAA Paper AIAA 2002-6020, 2002. doi:10.2514/6.2002-6020.

[7] John B Davidson, F. J. L., and Bundick, W. T., "Integrated Reconfigurable Control Allocation," *AIAA Guidance, Navigation, and Control Conference and Exhibit*, AIAA Paper 2001-4083, 2001. doi:10.2514/6.2001-4083.

[8] Wayne Durham, K. A. B., and Beck, R., *Aircraft Control Allocation*, AIAA Aerospace Series, Wiley, West Sussex, United Kingdom, 2017.

[9] Webster, R., *Convexity*, Oxford University Press, New York, 1994, Chaps. 1,2, pp. 45,65.

[10] Bernstein, D. S., and Haddad, W. M., *Control-System Synthesis: The Fixed-Structure Approach*, Self Published, 1995, Chap. 2, pp. 8–12.

[11] Arthur E. Bryson, J., and Ho, Y.-C., *Applied Optimal Control*, Taylor and Francis Group, New York, 1975, Chap. 1, pp. 6–10,27–28.